

Pricing energy spread options with variance gamma-driven Ornstein-Uhlenbeck dynamics

Tim Leung* Kevin Lu†

July 16, 2025

Abstract

We consider the pricing of energy spread options for spot prices following an exponential Ornstein-Uhlenbeck process driven by a sum of independent multivariate variance gamma processes. Within this class of mean-reverting, infinite activity price processes, the Esscher transform is used to obtain an equivalent martingale measure. We focus on the weak variance alpha-gamma process and show that it is not closed under the Esscher transform. By deriving an analytic expression for the cumulant generating function of the innovation term, we then obtain a pricing formula for forwards and apply the FFT method of Hurd and Zhou to price spread options. Lastly, we demonstrate how the model should be both estimated on energy prices under the real world measure and calibrated on forward or call prices, and provide numerical results for the pricing of spread options.

1 Introduction

Energy is a highly volatile commodity. Electricity markets in particular experience large price fluctuations due to temporary imbalances in supply and demand, weather events, unplanned power plant outages, and the intermittency of renewable energy generation. Retailers are exposed to this market risk as they buy electricity at the spot price and sell to customers at a fixed price. Energy derivatives are used to manage these risks, and this is the main topic of our study. A detailed monograph is provided by Benth, Šaltyté Benth and Koekebakker [8].

Specifically, we focus on the pricing of spread options, which are European-style derivatives on a bivariate price process (S_1, S_2) whose payoff is

$$f_T = (S_1(T) - S_2(T) - K)^+$$

*Department of Applied Mathematics, University of Washington, Seattle, WA, USA 98195. Email: timleung@uw.edu.

†Research School of Finance, Actuarial Studies & Statistics, Australian National University, Canberra ACT, Australia. kevin.lu@anu.edu.au.

with strike price K and maturity time T . Energy prices tend to be highly correlated across commodities and regions. For example, electricity prices are related to the price of gas used to generate it. An option on this difference is called a spark spread, which are used by generators to hedge against unanticipated spikes in production costs. As another example, the physical interconnectors between the five regions of the National Electricity Market in Australia also induce a correlation, and an option on such a difference would be a regional spread. The survey by Carmona and Durrleman [14] catalogs the variety of spread options. In general, there is no known closed-form pricing formula for spread options, except when $K = 0$ in a lognormal model where it reduces to the well-known Margrabe formula.

To approach this problem, we begin with the stylized facts that energy prices exhibit seasonality, mean reversion, and jumps. To account for these features, we assume that the n -dimensional energy spot price process $\mathbf{S} = (\mathbf{S}(t))_{t \in [0, T]}$ under the real world measure \mathbb{P} follows

$$\mathbf{S}(t) = \exp(\mathbf{\Lambda}(t) + \mathbf{X}(t)), \quad t \in [0, T], \quad (1.1)$$

where $\mathbf{\Lambda}(t)$ is a deterministic seasonality function, and \mathbf{X} is a Lévy-driven Ornstein-Uhlenbeck process (LDOUP) defined by

$$d\mathbf{X}(t) = -\lambda\mathbf{X}(t)dt + d\mathbf{Z}(\lambda t), \quad \mathbf{X}(0) = \mathbf{X}_0, \quad (1.2)$$

where \mathbf{Z} is the *background driving Lévy process (BDLP)*, $\lambda > 0$ is the speed of mean reversion, and the independent random vector \mathbf{X}_0 is the initial value. The Ornstein-Uhlenbeck part ensures mean reversion, while the Lévy part allows for jumps, and indeed the use of LDOUPs is widespread in energy price modeling. See for example [4, 8, 5, 16, 31].

The BDLP \mathbf{Z} we use herein is a sum of independent multivariate variance gamma (VG) processes with a focus on the weak variance alpha-gamma (WVAG) process by Buchmann, Lu and Madan [12] as a subclass. A multivariate VG process is a multivariate Brownian motion \mathbf{B} subordinated, or time-changed, by a univariate gamma subordinator, and such processes originated with Madan and Seneta [27] and have been studied in [11, 18]. While a sum of VG processes does not necessarily preserve such a time-change interpretation, the WVAG process being originally defined via weak subordination does. It turns out to be equivalent to a process \mathbf{Z} characterized in the following way: consider a subordinator \mathbf{T} which is a sum of G_k representing the idiosyncratic time-change for the k th price, and αG_0 representing a common time change for all prices, where G_0, \dots, G_n are independent gamma subordinators and $\alpha \in [0, \infty)^n$, then when $\mathbf{T}(t)$ jumps by $\Delta\mathbf{T}(t)$, $\mathbf{Z}(t)$ jumps by $\mathbf{B}(\Delta\mathbf{T}(t))$ in distribution, rather than pathwisely for traditional subordination. Consequently, the WVAG process, using weak subordination, preserves the essence of traditional subordination in a distributional or weak sense.

This provides a naturally multivariate process with a flexible dependence structure where the Brownian motion has arbitrary covariance in contrast to

other approaches, such as using traditional subordination restricted to independent Brownian motions to remain a Lévy process as considered by Luciano and Semeraro [25], or by summing independent univariate VG processes V_0, \dots, V_n in the form $\mathbf{Z} = (\alpha_1 V_0 + V_1, \dots, \alpha_n V_0 + V_n)$, an approach found in Ballotta and Bonfigliani [2], Caldana and Fusai [13], and Hurd and Zhou [22], with the latter two in the context of spread option pricing. Our BLDP \mathbf{Z} includes these cases. A similar way of summing univariate LDOUPs to produce a bivariate energy price for spread option pricing is also considered in [8, Section 9.2.1]. Our LDOUP \mathbf{X} include certain restrictions of this model, although both models are more general than each other in different ways.

So in all, our model of the multivariate energy spot prices allows for seasonality, mean reversion, has infinite activity due to the VG-related BDLP, and has a naturally multivariate time-change interpretation.

For the pricing of energy derivatives, we use the Esscher transform [20] to obtain an equivalent martingale measure (EMM) or Esscher measure $\mathbb{Q}_{\mathbf{h}}$ indexed by the market price of risk \mathbf{h} . This is a common approach for Lévy-based models, in which the market is incomplete due to the presence of jumps. Energy prices such as electricity are nontraded assets in the sense that term is used in standard arbitrage theory since electricity bought or sold on the market is instantly consumed and cannot be held to construct a replicating portfolio for the valuation of derivatives. Consequently, it is not assumed that the discounted energy price process is a $\mathbb{Q}_{\mathbf{h}}$ -martingale, a condition that would ordinarily determine a unique \mathbf{h} and hence an EMM $\mathbb{Q}_{\mathbf{h}}$ in an equity market. Instead, in an energy market, \mathbf{h} must be obtained by calibration, such as to observed forward and call prices.

Here, we show how the BDLP \mathbf{Z} changes under the Esscher transform into a sum of VG processes with modified parameters, which leads to the result that the class of WVAG processes is not closed under Esscher transform. In other related works, Buchmann et al. [11] studies Esscher transforms for a class of strongly subordinated Brownian motions, and Michaelsen and Szimayer [29] provides numerical results about pricing options on equities that follow a exponential WVAG process using the Esscher transform, although these rely on results that do not extend to energy derivatives. Our results are more general.

We derive an analytical formula for the cumulant generating function (cgf) of the innovation term of a LDOUP where the BLDP is a multivariate VG process in terms of the dilogarithm function, which generalizes a result in the univariate case by Sabino [31]. This is a key result given in Theorem 3.3, and is surprising in light of Remark 3.6. Consequently, we obtain an analytical formula for the cgf of the log return along with conditions for this to be finite and when it can be analytically continued into the complex plane. We use this cgf to obtain a forward pricing formula, and combined with the Fourier-based methods of Carr and Madan [15] and Hurd and Zhou [22], it also gives pricing formulas for call and spread options, respectively. This approach to pricing spread options differs from Benth and Šaltyté-Benth [7] where the spread is modelled directly as a univariate LDOUP as opposed to being based on (1.1). The Hurd-Zhou method has also been studied for spread options on equities and interest rates

in Alfeus and Schlögl [1].

For the WVAG BDLP, we provide numerical results under both the true model and the fitted model. Under the true model, the spread option price is computed via the analytical formula for the cgf of the log return with the FFT method, and is compared to the Monte Carlo method, showing close agreement. We also provide an end-to-end implementation of the spread option pricing in a simulation study by fitting the model. Our model allows the seasonality and LDOUP parameters to be estimated under the real world measure \mathbb{P} , specifically using the MLE method by Lu [24] combined with the analytical cgf of the log return, while the market price of risk \mathbf{h} is estimated under the Esscher measure $\mathbb{Q}_{\mathbf{h}}$, in the sense of calibrating the model to observed forward and call prices. Thus, we can coherently leverage both data on the \mathbb{P} -dynamics of the underlying and its derivative prices for model fitting, in contrast to the practice of fully calibrating the model under the risk-neutral measure for pricing energy derivatives [19, 31], and more commonly equity derivatives [26, 34]. Finally, the fitted model can be used to price spread options over a panel of strikes. We find in our example that calibrating to calls is better than calibrating to forwards, and demonstrate the extent to which errors in estimating the model parameters propagate to pricing errors.

The paper is organized as follows. Section 2 reviews the preliminaries, including notation, definitions of the VG and WVAG processes, and useful properties of LDOUPs. Section 3 presents the main probabilistic result, giving the analytical formula for the cgf of the innovation term of a LDOUP where the BDLP is multivariate VG. Section 4 focuses on the pricing of energy derivatives and is the main part of the paper, where we specify the model, show how the BDLP changes under the Esscher transform, obtain the analytical cgf of the log return, and finally apply this to derive pricing formulas for forwards, calls, and spread options. Section 5 details the implementation of our model and the pricing formulas, including simulation, estimation, calibration, and the pricing of spread options using the FFT method. Section 6 presents numerical results based on both the true parameters and a simulation study using fitted parameters. Section 7 concludes with some remarks on possible extensions.

2 Preliminaries

We use the convention that $\mathbf{x} = (x_1, \dots, x_n) \in \mathbb{R}^n$ represents a column vector. Let $\Sigma = (\Sigma_{ij})_{ij=1}^n \in \mathbb{R}^{n \times n}$ denote an $n \times n$ real matrix. For a multi-index α , define $[\cdot]_{\alpha}$ as extracting the α th element. For $A \subseteq \mathbb{R}^n$, let $\mathbf{1}_A$ be its indicator function and $A_* := A \setminus \{\mathbf{0}\}$. Let $\mathbb{D} := \{\mathbf{x} \in \mathbb{R}^n : \|\mathbf{x}\| \leq 1\}$. For $\mathbf{x}, \mathbf{y} \in \mathbb{R}^n$, define the Euclidean inner product $\langle \mathbf{x}, \mathbf{y} \rangle := \mathbf{x}'\mathbf{y}$, and $\|\mathbf{x}\|_{\Sigma} := \sqrt{\langle \mathbf{x}, \Sigma \mathbf{x} \rangle}$, which is a norm when Σ is positive definite. Let $\mathbf{e}_k \in \mathbb{R}^n$ be the k th standard basis vector. Let $I : [0, \infty) \rightarrow [0, \infty)$ be the identity function. The functions \exp and \log are understood to act componentwise on vectors so, for example, $e^{\mathbf{x}} = (e^{x_1}, \dots, e^{x_n})$.

Throughout, we work on the stochastic basis $(\Omega, \mathcal{F}, \mathbb{F}, \mathbb{P})$ with filtration $\mathbb{F} =$

$(\mathcal{F}_t)_{t \geq 0}$, where \mathbb{P} represents the real world measure. For now, let \mathbb{Q} be some probability measure equivalent to \mathbb{P} , which represents a risk-neutral measure.

We write a process \mathbf{X} in terms of its marginal components and time marginals by $\mathbf{X} = (X_1, \dots, X_n) = (\mathbf{X}(t))_{t \geq 0}$. Let $\stackrel{D}{=}$ denote equality in distribution or law. Let $\kappa_{\mathbf{X}}$, $\Psi_{\mathbf{X}}$ and $\Phi_{\mathbf{X}}$ denote respectively the cumulant generating function (cgf), characteristic exponent and characteristic function of the random vector \mathbf{X} , or of $\mathbf{X}(1)$ if \mathbf{X} is a process, under \mathbb{P} . Specifically, for a random vector \mathbf{X} , these are defined by

$$\kappa_{\mathbf{X}}(\boldsymbol{\theta}) := \log \mathbb{E}[e^{\langle \boldsymbol{\theta}, \mathbf{X} \rangle}], \quad \boldsymbol{\theta} \in \mathcal{D}_{\mathbf{X}},$$

where $\mathcal{D}_{\mathbf{X}} := \{\boldsymbol{\theta} \in \mathbb{R}^n : \mathbb{E}[e^{\langle \boldsymbol{\theta}, \mathbf{X} \rangle}] < \infty\}$ is the domain where \mathbf{X} has finite exponential moments, or equivalently, where $\kappa_{\mathbf{X}}$ is finite, and

$$\Phi_{\mathbf{X}}(\boldsymbol{\theta}) := \mathbb{E}[e^{i\langle \boldsymbol{\theta}, \mathbf{X} \rangle}] = e^{\Psi_{\mathbf{X}}(\boldsymbol{\theta})}, \quad \boldsymbol{\theta} \in \mathbb{R}^n.$$

Let $\kappa_{\mathbf{X}}^{\mathbb{Q}}$, $\Phi_{\mathbf{X}}^{\mathbb{Q}}$ and $\Psi_{\mathbf{X}}^{\mathbb{Q}}$ denote the respective functions under \mathbb{Q} . Let $\mathbf{B} \sim BM^n(\boldsymbol{\mu}, \boldsymbol{\Sigma})$ be an n -dimensional Brownian motion with drift $\boldsymbol{\mu} \in \mathbb{R}^n$ and covariance $\boldsymbol{\Sigma} \in \mathbb{R}^{n \times n}$. Let \circ denote the componentwise composition. For $\mathbf{t} = (t_1, \dots, t_n) \in [0, \infty)^n$, define

$$\boldsymbol{\mu} \diamond \mathbf{t} := (\mu_1 t_1, \dots, \mu_n t_n), \quad \boldsymbol{\Sigma} \diamond \mathbf{t} := (\Sigma_{ij}(t_i \wedge t_j))_{i,j=1}^n,$$

which are the mean vector and covariance matrix of $\mathbf{B} \circ \mathbf{t} = (B_1(t_1), \dots, B_n(t_n))$.

2.1 Variance gamma and related process

We begin with a summary of relevant definitions and results from the studies [11, 12]. Let $\Gamma_S(a, b)$ denote a univariate gamma subordinator with shape $a > 0$ and rate $b > 0$. An n -dimensional process $\mathbf{V} \sim VG^n(b, \boldsymbol{\mu}, \boldsymbol{\Sigma}, \boldsymbol{\eta})$ is a *variance gamma (VG) process* if

$$\mathbf{V} \stackrel{D}{=} \boldsymbol{\eta}I + \mathbf{B} \circ (G, \dots, G),$$

where $\mathbf{B} \sim BM^n(\boldsymbol{\mu}, \boldsymbol{\Sigma})$ and $G \sim \Gamma_S(b, b)$ are independent, and $\boldsymbol{\eta} \in \mathbb{R}^n$. The parameter $\boldsymbol{\eta}$ adds a drift. Whenever a process is written without a drift, such as $VG^n(b, \boldsymbol{\mu}, \boldsymbol{\Sigma})$, it is assumed that $\boldsymbol{\eta} = \mathbf{0}$. The VG process is a Lévy process with cgf

$$\kappa_{\mathbf{V}}(\boldsymbol{\theta}) = \langle \boldsymbol{\eta}, \boldsymbol{\theta} \rangle - b \log K_{\boldsymbol{\theta}}, \quad \boldsymbol{\theta} \in \mathcal{D}_{\mathbf{V}}, \quad (2.1)$$

where

$$K_{\boldsymbol{\theta}} := 1 - \frac{\langle \boldsymbol{\mu}, \boldsymbol{\theta} \rangle}{b} - \frac{\|\boldsymbol{\theta}\|_{\boldsymbol{\Sigma}}^2}{2b}, \quad (2.2)$$

$$\mathcal{D}_{\mathbf{V}} := \{\boldsymbol{\theta} \in \mathbb{R}^n : K_{\boldsymbol{\theta}} > 0\}. \quad (2.3)$$

It has characteristic exponent $\Psi_{\mathbf{V}}(\boldsymbol{\theta}) = \kappa_{\mathbf{V}}(i\boldsymbol{\theta})$, $\boldsymbol{\theta} \in \mathbb{R}^n$.

We define $\mathbf{Z} \sim VGC_m^n(\mathbf{b}, \boldsymbol{\mu}, \boldsymbol{\Sigma}, \boldsymbol{\eta})$ as a *VG convolution (VGC) or sum of VG processes* if

$$\mathbf{Z} \stackrel{D}{=} \boldsymbol{\eta}I + \mathbf{V}_1 + \cdots + \mathbf{V}_m, \quad (2.4)$$

where $\mathbf{V}_j \sim VG^n(b_j, \boldsymbol{\mu}_j, \boldsymbol{\Sigma}_j)$, $j = 1, \dots, m$, are mutually independent VG processes with $\mathbf{b} := (b_1, \dots, b_m)$, $\boldsymbol{\mu} := (\boldsymbol{\mu}_1, \dots, \boldsymbol{\mu}_m)$, $\boldsymbol{\Sigma} := (\boldsymbol{\Sigma}_1, \dots, \boldsymbol{\Sigma}_m)$ and $\boldsymbol{\eta} \in \mathbb{R}^n$. Clearly \mathbf{Z} is still a Lévy process.

Let $n \geq 2$, $a > 0$, $\boldsymbol{\alpha} = (\alpha_1, \dots, \alpha_n) \in (0, 1/a)^n$, $\beta_k := (1 - a\alpha_k)/\alpha_k$, $k = 1, \dots, n$, and $\boldsymbol{\eta} \in \mathbb{R}^n$. We define $\mathbf{Z} \sim WVAG^n(a, \boldsymbol{\alpha}, \boldsymbol{\mu}, \boldsymbol{\Sigma}, \boldsymbol{\eta})$ as a *weak variance alpha-gamma (WVAG)* process if

$$\mathbf{Z} \stackrel{D}{=} \boldsymbol{\eta}I + \mathbf{V}_0 + (V_1, \dots, V_n), \quad (2.5)$$

where $\mathbf{V}_0 \sim VG^n(a, a\boldsymbol{\mu} \diamond \boldsymbol{\alpha}, a\boldsymbol{\Sigma} \diamond \boldsymbol{\alpha})$ and $V_k \sim VG^1(\beta_k, \alpha_k \beta_k \mu_k, \alpha_k \beta_k \Sigma_{kk})$, $k = 1, \dots, n$, are independent. This representation allows us to see that the WVAG process is a sum of VG processes with $\mathbf{Z} \sim VGC_{n+1}^n(\mathbf{b}_S, \boldsymbol{\mu}_S, \boldsymbol{\Sigma}_S, \boldsymbol{\eta})$, where

$$\mathbf{b}_S = (a, \beta_1, \dots, \beta_n), \quad (2.6)$$

$$\boldsymbol{\mu}_S = (a\boldsymbol{\mu} \diamond \boldsymbol{\alpha}, \alpha_1 \beta_1 \mu_1 \mathbf{e}_1, \dots, \alpha_n \beta_n \mu_n \mathbf{e}_n), \quad (2.7)$$

$$\boldsymbol{\Sigma}_S = (a\boldsymbol{\Sigma} \diamond \boldsymbol{\alpha}, \alpha_1 \beta_1 \Sigma_{11} \mathbf{e}_1 \mathbf{e}'_1, \dots, \alpha_n \beta_n \Sigma_{nn} \mathbf{e}_n \mathbf{e}'_n), \quad (2.8)$$

which in turn allows the process to be simulated. The marginal components of $\mathbf{Z} = (Z_1, \dots, Z_n)$ are $Z_k \sim VG^1(1/\alpha_k, \mu_k, \Sigma_{kk}, \eta_k)$, which is a general univariate VG processes

It turns out that the original definition of WVAG process is not (2.5) but rather $\mathbf{Z} \stackrel{D}{=} \mathbf{B} \odot \mathbf{T}$, where $\mathbf{B} \sim BM^n(\boldsymbol{\mu}, \boldsymbol{\Sigma})$, \mathbf{T} is an n -dimensional alpha-gamma subordinator, and \odot is the weak subordination operation (see [12]), which gives it a multivariate time-change interpretation that is otherwise unclear in (2.5). Moreover, the original definition is equivalent to (2.5) for $\boldsymbol{\eta} = \mathbf{0}$.

2.2 Lévy-Driven Ornstein-Uhlenbeck Processes

Let $\mathbf{Z} \sim L^n(\boldsymbol{\mu}, \boldsymbol{\Sigma}, \mathcal{Z})$ denote an n -dimensional Lévy process with characteristic triplet $(\boldsymbol{\mu}, \boldsymbol{\Sigma}, \mathcal{Z})$, where $\boldsymbol{\mu} \in \mathbb{R}^n$, $\boldsymbol{\Sigma} \in \mathbb{R}^{n \times n}$ is a covariance matrix, and \mathcal{Z} is a Lévy measure. With reference to [24, 28, 32, 33], we recall that a Lévy-driven Ornstein-Uhlenbeck $\mathbf{X} \sim OU\text{-}\mathbf{Z}(\lambda)$ is defined by the SDE (1.2) for $t \geq 0$, where $\mathbf{Z} \sim L^n(\boldsymbol{\mu}, \boldsymbol{\Sigma}, \mathcal{Z})$ is the BDLP, $\lambda > 0$, and \mathbf{X}_0 is independent of \mathbf{Z} . Note that there is no loss in generality in having the drift term $-\lambda \mathbf{X}(t)dt$ instead of $\lambda(\bar{\boldsymbol{\mu}} - \mathbf{X}(t))dt$ for some $\bar{\boldsymbol{\mu}} \in \mathbb{R}^n$ since the stationary mean of \mathbf{X} is controlled by $\mathbb{E}[\mathbf{Z}(1)]$. There is also no loss in generality in having the Lévy term $d\mathbf{Z}(\lambda t)$ instead of $d\tilde{\mathbf{Z}}(t)$ for some general Lévy process $\tilde{\mathbf{Z}} \sim L^n(\tilde{\boldsymbol{\mu}}, \tilde{\boldsymbol{\Sigma}}, \tilde{\mathcal{Z}})$ since we can write $\tilde{\mathbf{Z}} \stackrel{D}{=} \mathbf{Z} \circ (\lambda I)$, where $\mathbf{Z} \sim L^n(\tilde{\boldsymbol{\mu}}/\lambda, \tilde{\boldsymbol{\Sigma}}/\lambda, \tilde{\mathcal{Z}}/\lambda)$.

The solution to the SDE (1.2) is

$$\mathbf{X}(t) = e^{-\lambda t} \mathbf{X}(s) + e^{-\lambda t} \int_s^t e^{\lambda u} d\mathbf{Z}(\lambda u), \quad 0 \leq s \leq t. \quad (2.9)$$

For $0 \leq s \leq t$, define the random vectors

$$\mathbf{Z}^*(s, t) := \int_s^t e^{\lambda u} d\mathbf{Z}(\lambda u), \quad \mathbf{Z}^*(t) := \mathbf{Z}^*(0, t).$$

This notation is from [36]. Note that

$$\mathbf{Z}^*(t) \stackrel{D}{=} \mathbf{Z}^*(s, s+t) \stackrel{D}{=} \int_0^{\lambda t} e^u d\mathbf{Z}(u) \quad (2.10)$$

for $s \geq 0$, $t \geq 0$, and $\mathbf{Z}^*(t)$ depends on λ . It then follows that equally spaced observations of the LDOUP at times $t_i = i\Delta$, $i = 0, 1, \dots, m$, with sampling interval $\Delta > 0$, forms an AR(1) process given by

$$\mathbf{X}(t_i) = b\mathbf{X}(t_{i-1}) + \mathbf{Z}_b^{(i)}, \quad i = 1, \dots, m, \quad (2.11)$$

where $b = e^{-\lambda\Delta}$, and $\mathbf{Z}_b^{(k)} \stackrel{D}{=} e^{-\lambda\Delta} \mathbf{Z}^*(\Delta)$ are the iid innovations. For convenience, we instead call $\mathbf{Z}^*(\Delta)$ the *innovation term*, and it has characteristic exponent is

$$\Psi_{\mathbf{Z}^*(t)}(\boldsymbol{\theta}) = \int_0^{\lambda t} \Psi_{\mathbf{Z}}(e^u \boldsymbol{\theta}) du, \quad \boldsymbol{\theta} \in \mathbb{R}^n \quad (2.12)$$

(see [33, Theorem 2.2]). This implies that if $\mathbf{Z} = \boldsymbol{\eta}I + \mathbf{Z}_1 + \dots + \mathbf{Z}_m$, where $\mathbf{Z}_1, \dots, \mathbf{Z}_m$ are independent Lévy processes, then

$$\Psi_{\mathbf{Z}^*(t)}(\boldsymbol{\theta}) = i\langle (e^{\lambda t} - 1)\boldsymbol{\eta}, \boldsymbol{\theta} \rangle + \sum_{j=1}^m \Psi_{\mathbf{Z}_j^*(t)}(\boldsymbol{\theta}). \quad (2.13)$$

We will use the VGC and WVAG processes as the BDLP. Specifically, we define a multivariate LDOUP $\mathbf{X} \sim OU-VGC_m^n(\lambda, \mathbf{b}, \boldsymbol{\mu}, \boldsymbol{\Sigma}, \boldsymbol{\eta})$ as an *OU-VGC process* if it has speed of mean reversion λ and BDLP $\mathbf{Z} \sim VGC_m^n(\mathbf{b}, \boldsymbol{\mu}, \boldsymbol{\Sigma}, \boldsymbol{\eta})$. In a similar way, the *OU-VG process* and *OU-WVAG process* are defined as having BDLPs $\mathbf{Z} \sim VG^n(b, \boldsymbol{\mu}, \boldsymbol{\Sigma}, \boldsymbol{\eta})$ and $\mathbf{Z} \sim WVAG^n(a, \boldsymbol{\alpha}, \boldsymbol{\mu}, \boldsymbol{\Sigma}, \boldsymbol{\eta})$, respectively. Since the marginal component of a multivariate LDOUP is a univariate LDOUP, it follows that if $\mathbf{X} \sim OU-WVAG^n(\lambda, a, \boldsymbol{\alpha}, \boldsymbol{\mu}, \boldsymbol{\Sigma}, \boldsymbol{\eta})$, then it has k th marginal component $X_k \sim OU-VG^1(\lambda, 1/\alpha_k, \mu_k, \Sigma_{kk}, \eta_k)$.

3 Analytical formula for cgf of the innovation term

Our main result is the analytical formula for the cgf of the innovation term $\mathbf{V}^*(t)$, $t > 0$, of a multivariate OU-VG process.

This formula, which will later be applied under both \mathbb{P} and $\mathbb{Q}_{\mathbf{h}}$, has 3 applications in the pricing of energy derivatives. First, in the univariate and bivariate setting under \mathbb{P} , it is used in the likelihood function to estimate the LDOUP parameters (see Section 5.3). Second, in the univariate setting under $\mathbb{Q}_{\mathbf{h}}$, it is used to price forwards (see Section 4.4.1), calls (see Section 4.4.2), and calibrate the model (see Section 5.4). Third, in the bivariate setting under $\mathbb{Q}_{\mathbf{h}}$, it is used to price spread options (see Sections 4.4.3 and 5.5).

To begin, for a general $\mathbf{X} \sim OU\text{-}\mathbf{Z}(\lambda)$, $\lambda > 0$, we give a lemma to deal with finiteness of the cgf, which is a version of [6, Lemma 4.1] adapted to our setting with a slightly different proof.

Lemma 3.1. *Let $\mathbf{Z} \sim L^n(\boldsymbol{\mu}, \boldsymbol{\Sigma}, \mathcal{Z})$ and $t > 0$. Let $\mathcal{D}_{\mathbf{Z}^*(t)} = e^{-\lambda t} \mathcal{D}_{\mathbf{Z}}$. If $\boldsymbol{\theta} \in \mathcal{D}_{\mathbf{Z}^*(t)}$, then*

$$\kappa_{\mathbf{Z}^*(t)}(\boldsymbol{\theta}) = \int_0^{\lambda t} \kappa_{\mathbf{Z}}(e^s \boldsymbol{\theta}) ds \quad (3.1)$$

is finite, and also $\kappa_{\mathbf{Z}}(e^s \boldsymbol{\theta})$ is finite for all $s \in [0, \lambda t]$. Furthermore, (3.1) holds for all $\boldsymbol{\theta} \in \mathbb{C}^n$ such that $\text{Re}(\boldsymbol{\theta}) \in \mathcal{D}_{\mathbf{Z}}$.

Proof. The random vector $\mathbf{Z}^*(t)$ is infinitely divisible, and by using the Lévy measure of $e^{-\lambda t} \tilde{\mathbf{Z}}^*(t)$, where $\tilde{\mathbf{Z}} = \mathbf{Z} \circ (\lambda I)$, given by [32, Lemma 17.1], it follows that the Lévy measure of $\mathbf{Z}^*(t)$ is

$$\mathcal{Z}^*(B) = \int_{\mathbb{R}_*^n} \int_0^t \lambda \mathbf{1}_{e^{\lambda t} B}(e^{-\lambda s} \mathbf{z}) ds \mathcal{Z}(d\mathbf{z}), \quad B \in \mathcal{B}(\mathbb{R}_*^n),$$

using [32, Proposition 11.10].

Let $\boldsymbol{\theta} \in \mathcal{D}_{\mathbf{Z}^*(t)}$, or equivalently $e^{\lambda t} \boldsymbol{\theta} \in \mathcal{D}_{\mathbf{Z}}$. By the change of variables $u = \lambda(t - s)$ and Tonelli's theorem,

$$\begin{aligned} I &:= \int_{\mathbb{D}^C} e^{\langle \boldsymbol{\theta}, \mathbf{z} \rangle} \mathcal{Z}^*(d\mathbf{z}) = \int_{\mathbb{D}^C} \int_0^{\lambda t} e^{\langle \boldsymbol{\theta}, e^u \mathbf{z} \rangle} du \mathcal{Z}(d\mathbf{z}) \\ &= \int_0^{\lambda t} \int_{\mathbb{D}^C} e^{\langle e^u \boldsymbol{\theta}, \mathbf{z} \rangle} \mathcal{Z}(d\mathbf{z}) du. \end{aligned} \quad (3.2)$$

By the exponential moment theorem (see [32, Theorem 25.17]), $\mathcal{D}_{\mathbf{Z}}$ is a convex set containing $\mathbf{0}$, so that $e^{\lambda t} \boldsymbol{\theta} \in \mathcal{D}_{\mathbf{Z}}$ implies $e^u \boldsymbol{\theta} \in \mathcal{D}_{\mathbf{Z}}$ for all $u \in [0, \lambda t]$, and hence

$$f(u) := \int_{\mathbb{D}^C} e^{\langle e^u \boldsymbol{\theta}, \mathbf{z} \rangle} \mathcal{Z}(d\mathbf{z}) < \infty$$

for all $u \in [0, \lambda t]$. Next, by a version of the dominated convergence theorem (see [3, Lemma 16.1]) using $\mathbf{z} \mapsto 1 + e^{\langle e^{\lambda t} \boldsymbol{\theta}, \mathbf{z} \rangle}$ as the dominating function and the definition of the Lévy measure for \mathcal{Z} , it follows that f is continuous on $[0, \lambda t]$. Thus, $I < \infty$, so that $\kappa_{\mathbf{Z}^*(t)}(\boldsymbol{\theta})$ is finite for all $\boldsymbol{\theta} \in \mathcal{D}_{\mathbf{Z}^*(t)}$ by the exponential moment theorem.

Lastly, by infinite divisibility, (2.12) has Lévy-Khintchine representation that can now be analytically continued by the exponential moment theorem so that (3.1) holds for all $\boldsymbol{\theta} \in \mathbb{C}^n$ such that $\text{Re}(\boldsymbol{\theta}) \in \mathcal{D}_{\mathbf{Z}^*(t)}$. \square

Remark 3.2. Note that $\boldsymbol{\theta} \in \mathcal{D}_{\mathbf{Z}^*(t)}$ is equivalent to $e^{\lambda t} \boldsymbol{\theta} \in \mathcal{D}_{\mathbf{Z}}$. If this holds, then $\kappa_{\mathbf{Z}^*(t)}(\boldsymbol{\theta})$ is finite. Following the proof and considering (3.2), we see that if $e^{\lambda t} \boldsymbol{\theta} \notin \text{cl}(\mathcal{D}_{\mathbf{Z}})$, where cl is the closure, then $\kappa_{\mathbf{Z}^*(t)}(\boldsymbol{\theta})$ is not finite, but if $e^{\lambda t} \boldsymbol{\theta} \in \partial(\mathcal{D}_{\mathbf{Z}})$, where ∂ is the boundary, it is unclear whether $\kappa_{\mathbf{Z}^*(t)}(\boldsymbol{\theta})$ is finite or not, as only one endpoint of the integrand is infinite. Accordingly, all sets of the form $\mathcal{D}_{\mathbf{Z}^*(t)}$ should be understood in the sense that $\mathcal{D}_{\mathbf{Z}^*(t)} \subseteq \{\boldsymbol{\theta} \in \mathbb{R}^n : \mathbb{E}[e^{\langle \boldsymbol{\theta}, \mathbf{Z}^*(t) \rangle}] < \infty\}$. \square

Let Li_2 denote the dilogarithm function [37], which is defined by

$$\text{Li}_2(z) = \int_0^z -\frac{\log(1-y)}{y} dy,$$

where $z \in \mathbb{C} \setminus [1, \infty)$. Provided that $z \leq 1$, $\text{Li}_2(z) \in \mathbb{R}$ with $\text{Li}_2(1) = \pi^2/6$. Now we give the analytical formula for the cgf of $\mathbf{V}^*(t)$ using a method inspired by [31].

Theorem 3.3. *Let $\mathbf{V} \sim VG^n(b, \boldsymbol{\mu}, \boldsymbol{\Sigma})$ and $t > 0$. Let $\mathcal{D}_{\mathbf{V}^*(t)} = e^{-\lambda t} \mathcal{D}_{\mathbf{V}}$. If $\boldsymbol{\theta} \in \mathcal{D}_{\mathbf{V}^*(t)}$, then*

$$\kappa_{\mathbf{V}^*(t)}(\boldsymbol{\theta}) = \begin{cases} b[\text{Li}_2(e^{\lambda t} A(\boldsymbol{\theta})) - \text{Li}_2(A(\boldsymbol{\theta})) \\ \quad + \text{Li}_2(-e^{\lambda t} B(\boldsymbol{\theta})) - \text{Li}_2(-B(\boldsymbol{\theta}))], & \text{if } \|\boldsymbol{\theta}\|_{\boldsymbol{\Sigma}}^2 > 0, \\ b(\text{Li}_2(e^{\lambda t} \tilde{A}(\boldsymbol{\theta})) - \text{Li}_2(\tilde{A}(\boldsymbol{\theta}))), & \text{if } \|\boldsymbol{\theta}\|_{\boldsymbol{\Sigma}}^2 = 0, \end{cases} \quad (3.3)$$

where

$$A(\boldsymbol{\theta}) = \frac{\sqrt{\langle \boldsymbol{\mu}, \boldsymbol{\theta} \rangle^2 + 2b\|\boldsymbol{\theta}\|_{\boldsymbol{\Sigma}}^2} + \langle \boldsymbol{\mu}, \boldsymbol{\theta} \rangle}{2b}, \quad B(\boldsymbol{\theta}) = \frac{\sqrt{\langle \boldsymbol{\mu}, \boldsymbol{\theta} \rangle^2 + 2b\|\boldsymbol{\theta}\|_{\boldsymbol{\Sigma}}^2} - \langle \boldsymbol{\mu}, \boldsymbol{\theta} \rangle}{2b},$$

and $\tilde{A}(\boldsymbol{\theta}) = \langle \boldsymbol{\mu}, \boldsymbol{\theta} \rangle / b$. Furthermore, (3.3) holds for all $\boldsymbol{\theta} \in \mathbb{C}^n$ such that $\text{Re}(\boldsymbol{\theta}) \in \mathcal{D}_{\mathbf{V}^*(t)}$.

Proof. Let $\boldsymbol{\theta} \in \mathcal{D}_{\mathbf{V}^*(t)}$ defined in Lemma 3.1. Consider the $\|\boldsymbol{\theta}\|_{\boldsymbol{\Sigma}}^2 > 0$ case. Let $A := A(\boldsymbol{\theta})$, $B := B(\boldsymbol{\theta})$, $c := e^{\lambda t}$. Notice that

$$M(u) := 1 - \frac{\langle \boldsymbol{\mu}, \boldsymbol{\theta} \rangle}{b} u - \frac{\|\boldsymbol{\theta}\|_{\boldsymbol{\Sigma}}^2}{2b} u^2 = (1 - Au)(1 + Bu).$$

By Lemma 3.1, $\kappa_{\mathbf{V}^*(t)}(\boldsymbol{\theta})$ is finite and

$$\kappa_{\mathbf{V}^*(t)}(\boldsymbol{\theta}) = -b \int_1^c \frac{\log M(u)}{u} du \quad (3.4)$$

$$= -b \int_1^c \frac{\log(1 - Au)}{u} + \frac{\log(1 + Bu)}{u} du \quad (3.5)$$

$$= b \int_A^{cA} -\frac{\log(1-y)}{y} dy + \int_{-B}^{-cB} -\frac{\log(1-y)}{y} dy, \quad (3.6)$$

which gives (3.3).

We now check that the above expressions are defined. Firstly, according to Lemma 3.1, $M(e^s) > 0$ for $s \in [0, \lambda t]$, or equivalently $M(u) > 0$ for $u \in [1, c]$, so (3.4) is defined. The coefficient of u^2 in $M(u)$ satisfies $AB = \|\boldsymbol{\theta}\|_{\Sigma}^2 / (2b) > 0$. Clearly $A > 0$, so we must have $B > 0$. Now either both $1 - Au$ and $1 + Bu$ are strictly positive for all $u \in [1, c]$, or strictly negative. However, $1 + Bu < 0$ is impossible since $u < -1/B < 0$ contradicts $u \geq 1$. Thus, we must have $1 - Au > 0$ and $1 + Bu > 0$ for all $u \in [1, c]$, so (3.5) is defined. Observe that $-cB < B \leq A < cA < 1$, where the last inequality is implied by $1 - Au > 0$ on $u \in [1, c]$. Thus, we have ensured (3.6) can be evaluated using Li_2 on the subset of the domain where the function is real.

Finally, the $\|\boldsymbol{\theta}\|_{\Sigma}^2 = 0$ case follows from similar arguments by noting that, with $\tilde{A} := \tilde{A}(\boldsymbol{\theta})$, we have $M(u) = 1 - \tilde{A}u > 0$ on $u \in [1, c]$ and $c\tilde{A} < 1$. \square

Remark 3.4. If $\boldsymbol{\theta} = \mathbf{0}$, then $\kappa_{\mathbf{V}^*(t)}(\boldsymbol{\theta}) = 0$. If the covariance matrix Σ is invertible, or equivalently positive definite, and $\boldsymbol{\theta} \neq \mathbf{0}$, then only the $\|\boldsymbol{\theta}\|_{\Sigma}^2 > 0$ case in (3.3) holds, and the other case is impossible. Also, $\kappa_{\mathbf{V}^*(0)}(\boldsymbol{\theta}) = 0$, $\boldsymbol{\theta} \in \mathcal{D}_{\mathbf{V}^*(0)} = \mathbb{R}^n$. Finally, as $\mathbf{0} \in \mathcal{D}_{\mathbf{V}^*(t)}$, the last part of Theorem 3.3 gives the characteristic exponent $\Psi_{\mathbf{V}^*(t)}(\boldsymbol{\theta}) = \kappa_{\mathbf{V}^*(t)}(i\boldsymbol{\theta})$, $\boldsymbol{\theta} \in \mathbb{R}^n$. \square

Corollary 3.5. *Let $V \sim VG^1(b, \mu, \Sigma)$, $\Sigma > 0$, and $t > 0$. Let $\mathcal{D}_{\mathbf{V}^*(t)} = e^{-\lambda t} \mathcal{D}_V$. If $\theta \in \mathcal{D}_{\mathbf{V}^*(t)}$, then*

$$\kappa_{\mathbf{V}^*(t)}(\theta) = b[\text{Li}_2(e^{\lambda t} A(\theta)) - \text{Li}_2(A(\theta)) + \text{Li}_2(-e^{\lambda t} B(\theta)) - \text{Li}_2(-B(\theta))], \quad (3.7)$$

where

$$A(\theta) = \frac{\sqrt{\mu^2 + 2b\Sigma}}{2b} |\theta| + \frac{\mu\theta}{2b}, \quad B(\theta) = \frac{\sqrt{\mu^2 + 2b\Sigma}}{2b} |\theta| - \frac{\mu\theta}{2b}. \quad (3.8)$$

Remark 3.6. The formula for $\kappa_{\mathbf{V}^*(t)}(\theta)$ in univariate case was already obtained in Sabino [31, Equation (18)]. Sabino's proof is based on the well-known fact that the VG process $V \stackrel{D}{=} G^+ - G^-$ is the difference of two independent gamma subordinators since its characteristic exponent is $\Psi_V(\theta) = \Psi_{G^+}(\theta) + \Psi_{G^-}(-\theta)$, where

$$\Psi_{G^\pm}(\theta) = -b \log \left(1 - i \frac{\sqrt{\mu^2 + 2b\Sigma} \theta \pm \mu\theta}{2b} \right), \quad \theta \in \mathbb{R}.$$

This is why Sabino's formula has $|\theta|$ in (3.8) replaced with θ but is otherwise the same. Numerically, this causes the arguments of Li_2 to be different despite the value of $\kappa_{\mathbf{V}^*(t)}(\theta)$ being the same.

As noted in [24, Remark 7], Sabino's proof did not seem to readily extend as it has no multivariate analog. Specifically, the multivariate VG process \mathbf{V}

cannot be written as a difference of multivariate gamma processes as it is not in the class of generalized gamma convolutions provided that Σ is invertible. This makes Theorem 3.3 quite surprising. In fact, using methods similar to the proof allows us to write $\Psi_{\mathbf{V}}(\boldsymbol{\theta}) = \Psi_{\mathbf{G}^+}(\boldsymbol{\theta}) + \Psi_{\mathbf{G}^-}(-\boldsymbol{\theta})$, where

$$\Psi_{\mathbf{G}^\pm}(\boldsymbol{\theta}) = -b \log \left(1 - i \frac{\sqrt{\langle \boldsymbol{\mu}, \boldsymbol{\theta} \rangle^2 + 2b \|\boldsymbol{\theta}\|_{\Sigma}^2} \pm \langle \boldsymbol{\mu}, \boldsymbol{\theta} \rangle}{2b} \right), \quad \boldsymbol{\theta} \in \mathbb{R}^n,$$

which raises the question of whether \mathbf{V} can be written as the difference of two other Lévy processes \mathbf{G}^\pm with characteristic exponents $\Psi_{\mathbf{G}^\pm}(\boldsymbol{\theta})$. Unfortunately, the answer is no as $\Psi_{\mathbf{G}^\pm}(\boldsymbol{\theta})$ is not a valid characteristic exponent. If it were, then its first marginal component G_1^\pm would have characteristic exponent

$$\Psi_{G_1^\pm}(\theta_1) = -b \log \left(1 - i \frac{\sqrt{\mu_1^2 + 2b \Sigma_{11}} |\theta_1| \pm \mu_1 \theta_1}{2b} \right), \quad \theta_1 \in \mathbb{R},$$

but $\Phi_{G_1^+}(\theta_1)$ fails to be a characteristic function because it can fail to satisfy the necessary condition $\Phi_{G_1^+}(-\theta_1) = \overline{\Phi_{G_1^+}(\theta_1)}$. \square

4 Energy derivatives

In this section, we specify our energy market model using a LDOUP, show how a risk-neutral measure can be obtained by the Esscher transform, and how forward contracts, call options and spread options can be priced.

4.1 Energy market model

We define a market model on $(\Omega, \mathcal{F}, \mathbb{F}, \mathbb{P})$ with finite time horizon T , filtration $\mathbb{F} = (\mathcal{F}_t)_{t \in [0, T]}$, and real world measure \mathbb{P} .

Let $\boldsymbol{\Lambda} = (\boldsymbol{\Lambda}(t))_{t \in [0, T]}$ be a deterministic *seasonality function* with k th marginal component

$$\Lambda_k(t) = b_{0k} + b_{1k}t + b_{2k} \cos\left(\frac{2\pi}{p}t\right) + b_{3k} \sin\left(\frac{2\pi}{p}t\right), \quad t \in [0, T],$$

$k = 1, \dots, n$, where p is the period, and $b_{0k}, b_{1k}, b_{2k}, b_{3k} \in \mathbb{R}$. Let $\mathbf{X} \sim OU-VGC_m^n(\lambda, \mathbf{b}, \boldsymbol{\mu}, \Sigma, \boldsymbol{\eta})$ with initial value \mathbf{X}_0 in its stationary distribution. Thus, the BDLP is $\mathbf{Z} \sim VGC_m^n(\mathbf{b}, \boldsymbol{\mu}, \Sigma, \boldsymbol{\eta})$, and we work within this more general setting throughout, which includes $\mathbf{Z} \sim WVAG^n(a, \boldsymbol{\alpha}, \boldsymbol{\mu}, \Sigma, \boldsymbol{\eta})$ as a subclass. In Section 5.1, we make an additional assumption on $\boldsymbol{\eta}$, which is not needed now.

Recalling (1.1), the n -dimensional energy spot price process $\mathbf{S} = (\mathbf{S}(t))_{t \in [0, T]}$ is defined by the log price process

$$\mathbf{Y}(t) := \log \mathbf{S}(t) = \boldsymbol{\Lambda}(t) + \mathbf{X}(t). \quad (4.1)$$

We assume \mathbf{Z} , or equivalently \mathbf{S} , is adapted to \mathbb{F} . Also, define the log return over time interval $[s, t]$ as

$$\mathbf{R}(s, t) := \mathbf{Y}(t) - \mathbf{Y}(s).$$

In this model, \mathbf{S} is not a traded asset. The only traded asset is the risk-free asset, which has constant risk-free rate r .

We use a geometric model which ensures prices are positive. While electricity often exhibits negative intraday prices, derivative pricing is usually based on average daily price data (for example, see [9, Section 3], [6, Section 3], [8, Section 9.3.2]), which are almost always positive.

4.2 Esscher transform

We now use the Esscher transform to obtain an EMM. For references on Esscher transforms and its applications to derivative pricing in equity markets see [20, 21], [30, Section 13.5], [35, Section VII.3c], and for applications to energy markets, see [8].

Let $\mathbf{Z} \sim L^n$ be a Lévy process. The *Esscher measure* $\mathbb{Q}_{\mathbf{h}}$ of \mathbf{Z} with Esscher parameter or *market price of risk (MPR)* $\mathbf{h} = (h_1, \dots, h_n)$ is defined by the Radon-Nikodym derivative

$$\frac{d\mathbb{Q}_{\mathbf{h}}}{d\mathbb{P}} \Big|_{\mathcal{F}_t} = \frac{e^{\langle \mathbf{h}, \mathbf{Z}(t) \rangle}}{\mathbb{E}[e^{\langle \mathbf{h}, \mathbf{Z}(t) \rangle}]} \quad (4.2)$$

It is immediate that $\mathbb{Q}_{\mathbf{h}}$ exists if and only if $\mathbf{h} \in \mathcal{D}_{\mathbf{Z}}$ and it is equivalent to \mathbb{P} . The Esscher transform is structure preserving in the sense that \mathbf{Z} is also a Lévy process under $\mathbb{Q}_{\mathbf{h}}$, where \mathbf{h} is commonly called the *market price of risk (MPR)*.

The no arbitrage condition that the discounted traded asset prices are $\mathbb{Q}_{\mathbf{h}}$ -martingales trivially holds for the risk-free asset, which is the only traded asset, so that the Esscher transform provides up to infinitely many EMMs $\mathbb{Q}_{\mathbf{h}}$ indexed by $\mathbf{h} \in \mathcal{D}_{\mathbf{Z}}$, all consistent with no arbitrage. The market chooses a MRP $\mathbf{h} \in \mathcal{D}_{\mathbf{Z}}$ based on risk preferences, which we infer by calibrating the model to observed forward and call prices.

We now give some results on the $\mathbb{Q}_{\mathbf{h}}$ -dynamics of the BDLP \mathbf{Z} , which by equivalence determines the $\mathbb{Q}_{\mathbf{h}}$ -dynamics of \mathbf{S} . We begin with the case where the BDLP is multivariate VG. While the univariate case can be found in [21, Proposition 4], the multivariate case does not appear to be readily available except in [10, Theorem 6.3.1], and we reproduce this proof below. However, it is also an implication of [11, Theorem 2.16].

Lemma 4.1. *Suppose $\mathbf{V} \sim VG^n(b, \boldsymbol{\mu}, \boldsymbol{\Sigma})$ under \mathbb{P} . If $\mathbf{h} \in \mathcal{D}_{\mathbf{V}}$, then $\mathbf{V} \sim VG^n(b_{\mathbf{h}}, \boldsymbol{\mu}_{\mathbf{h}}, \boldsymbol{\Sigma}_{\mathbf{h}})$ under $\mathbb{Q}_{\mathbf{h}}$, where*

$$b_{\mathbf{h}} = b, \quad \boldsymbol{\mu}_{\mathbf{h}} = \frac{\boldsymbol{\mu} + \boldsymbol{\Sigma}\mathbf{h}}{K_{\mathbf{h}}}, \quad \boldsymbol{\Sigma}_{\mathbf{h}} = \frac{\boldsymbol{\Sigma}}{K_{\mathbf{h}}}, \quad (4.3)$$

and $K_{\mathbf{h}}$ is defined in (2.2).

Proof. Let $\mathbf{h} \in \mathcal{D}_{\mathbf{V}}$, then there always exists an open neighborhood $U \subseteq \mathbb{R}^n$ about $\mathbf{0}$ such that if $\boldsymbol{\theta} \in U$, then $\boldsymbol{\theta} + \mathbf{h} \in \mathcal{D}_{\mathbf{V}}$. The moment generating function of \mathbf{V} under $\mathbb{Q}_{\mathbf{h}}$ is

$$\begin{aligned} M_{\mathbf{V}}^{\mathbb{Q}_{\mathbf{h}}}(\boldsymbol{\theta}) &= \mathbb{E}_{\mathbb{Q}_{\mathbf{h}}} \left[e^{\langle \boldsymbol{\theta}, \mathbf{V}(1) \rangle} \frac{e^{\langle \mathbf{h}, \mathbf{V}(1) \rangle}}{\mathbb{E}[e^{\langle \mathbf{h}, \mathbf{V}(1) \rangle}]} \right] \\ &= \frac{e^{\kappa_{\mathbf{V}}(\boldsymbol{\theta} + \mathbf{h})}}{e^{\kappa_{\mathbf{V}}(\boldsymbol{\theta})}} \\ &= \left(\frac{b - \langle \boldsymbol{\mu}, \mathbf{h} \rangle - \frac{1}{2} \|\mathbf{h}\|_{\boldsymbol{\Sigma}}^2}{b - \langle \boldsymbol{\mu}, \mathbf{h} \rangle - \frac{1}{2} \|\mathbf{h}\|_{\boldsymbol{\Sigma}}^2 - \langle \boldsymbol{\mu} + \boldsymbol{\Sigma} \mathbf{h}, \boldsymbol{\theta} \rangle - \frac{1}{2} \|\boldsymbol{\theta}\|_{\boldsymbol{\Sigma}}^2} \right)^b \\ &= \left(\frac{b_{\mathbf{h}}}{b_{\mathbf{h}} - \langle \boldsymbol{\mu}_{\mathbf{h}}, \boldsymbol{\theta} \rangle - \frac{1}{2} \|\boldsymbol{\theta}\|_{\boldsymbol{\Sigma}_{\mathbf{h}}}^2} \right)^b \end{aligned}$$

using (4.2) in the first line, (2.1) in the third line, and (4.3) in the last line. As this coincides with the moment generating function of $VG^n(b_{\mathbf{h}}, \boldsymbol{\mu}_{\mathbf{h}}, \boldsymbol{\Sigma}_{\mathbf{h}})$ on U , the result follows. \square

Note that $\mathcal{D}_{\mathbf{V}}$ is defined in (2.3) using the parameters $(b, \boldsymbol{\mu}, \boldsymbol{\Sigma})$ under \mathbb{P} . This is always the case, including similarly for the proceeding results.

We see that the existence of the Esscher measure $\mathbb{Q}_{\mathbf{h}}$ depends importantly on \mathbf{h} and the kurtosis parameter $b > 0$. For any choice of $(b, \boldsymbol{\mu}, \boldsymbol{\Sigma})$, if $\|\mathbf{h}\|$ is sufficiently small, then $K_{\mathbf{h}} > 0$, which is equivalent to $\mathbf{h} \in \mathcal{D}_{\mathbf{V}}$ and $\mathbb{Q}_{\mathbf{h}}$ existing. Alternatively, for any choice of \mathbf{h} , if b is sufficiently large, so that the kurtosis is sufficiently small, then $K_{\mathbf{h}} > 0$. Otherwise, for an arbitrary choice of $(b, \boldsymbol{\mu}, \boldsymbol{\Sigma})$ and \mathbf{h} , $\mathbb{Q}_{\mathbf{h}}$ may not exist.

Let $p_{\mathbf{h}}$ denote the map sending the \mathbb{P} parameter to the $\mathbb{Q}_{\mathbf{h}}$ parameters for the VG process, so $p_{\mathbf{h}}(b, \boldsymbol{\mu}, \boldsymbol{\Sigma}) = (b_{\mathbf{h}}, \boldsymbol{\mu}_{\mathbf{h}}, \boldsymbol{\Sigma}_{\mathbf{h}})$.

Corollary 4.2. *Suppose $\mathbf{Z} \sim VGC_m^n(\mathbf{b}, \boldsymbol{\mu}, \boldsymbol{\Sigma}, \boldsymbol{\eta})$ under \mathbb{P} is written as*

$$\mathbf{Z} \stackrel{D}{=} \boldsymbol{\eta}I + \mathbf{V}_1 + \cdots + \mathbf{V}_m.$$

from (2.4). If $\mathbf{h} \in \mathcal{D}_{\mathbf{Z}}$, then this holds under $\mathbb{Q}_{\mathbf{h}}$ with $\mathbf{Z} \sim VGC_m^n(\mathbf{b}_{\mathbf{h}}, \boldsymbol{\mu}_{\mathbf{h}}, \boldsymbol{\Sigma}_{\mathbf{h}}, \boldsymbol{\eta})$, where $\mathbf{V}_j \sim VG^n([\mathbf{b}_{\mathbf{h}}]_j, [\boldsymbol{\mu}_{\mathbf{h}}]_j, [\boldsymbol{\Sigma}_{\mathbf{h}}]_j)$, $j = 1, \dots, m$, are independent, and

$$([\mathbf{b}_{\mathbf{h}}]_j, [\boldsymbol{\mu}_{\mathbf{h}}]_j, [\boldsymbol{\Sigma}_{\mathbf{h}}]_j) = p_{\mathbf{h}}(b_j, \boldsymbol{\mu}_j, \boldsymbol{\Sigma}_j),$$

and

$$\mathcal{D}_{\mathbf{Z}} = \bigcap_{j=1}^m \mathcal{D}_{\mathbf{V}_j}. \quad (4.4)$$

Proof. Without loss of generality, suppose $\boldsymbol{\eta} = \mathbf{0}$. Let $\mathbf{h} \in \mathcal{D}_{\mathbf{Z}}$. Combining [35, Section VII.2c, Theorem 1], that $\mathbf{V}_1, \dots, \mathbf{V}_m$ are independent under \mathbb{P} , and Kac's theorem, it follows that $\mathbf{V}_1, \dots, \mathbf{V}_m$ are independent under $\mathbb{Q}_{\mathbf{h}}$. Specifically, with $\tilde{\mathbf{V}} := (\mathbf{V}_1, \dots, \mathbf{V}_m)$, this claim follows from

$$\begin{aligned}
\kappa_{\tilde{\mathbf{V}}}^{\mathbb{Q}_{\mathbf{h}}}(\boldsymbol{\theta}_1, \dots, \boldsymbol{\theta}_m) &= \kappa_{\tilde{\mathbf{V}}}(\boldsymbol{\theta}_1 + \mathbf{h}, \dots, \boldsymbol{\theta}_m + \mathbf{h}) - \kappa_{\tilde{\mathbf{V}}}(\mathbf{h}, \dots, \mathbf{h}) \\
&= \sum_{j=1}^m \kappa_{\mathbf{V}_j}(\boldsymbol{\theta}_j + \mathbf{h}) - \kappa_{\mathbf{V}_j}(\mathbf{h}) \\
&= \sum_{j=1}^m \kappa_{\mathbf{V}_j}^{\mathbb{Q}_{\mathbf{h}}}(\boldsymbol{\theta}_j),
\end{aligned}$$

where as in the proof of Lemma 4.1, there exists a neighborhood $U_j \subseteq \mathbb{R}^n$ about $\mathbf{0}$, such that $\boldsymbol{\theta}_j \in U_j$ and $\boldsymbol{\theta}_j + \mathbf{h} \in \mathcal{D}_{\mathbf{V}_j}$ for all $j = 1, \dots, m$. Also, note that (4.4) holds since $\mathbb{E}[e^{\langle (\boldsymbol{\theta}_1, \dots, \boldsymbol{\theta}_m), \tilde{\mathbf{V}} \rangle}] = \prod_{j=1}^m \mathbb{E}[e^{\langle \boldsymbol{\theta}_j, \mathbf{V}_j \rangle}]$ with the LHS finite if and only if each term in the product is, otherwise both sides are infinite.

Thus, applying Lemma 4.1 to each \mathbf{V}_j completes the proof. \square

Note that all but the last line of this proof shows the fact that the Esscher transform preserves independence and is applicable to any Lévy processes.

Corollary 4.3. *Suppose $\mathbf{Z} \sim WVAG^n(a, \boldsymbol{\alpha}, \boldsymbol{\mu}, \boldsymbol{\Sigma}, \boldsymbol{\eta})$ under \mathbb{P} is written as*

$$\mathbf{Z} \stackrel{D}{=} \boldsymbol{\eta}I + \mathbf{V}_0 + (V_1, \dots, V_n)$$

from (2.5). If $\mathbf{h} \in \mathcal{D}_{\mathbf{Z}}$, then this holds under $\mathbb{Q}_{\mathbf{h}}$, where $\mathbf{V}_0 \sim VG^n(a, \boldsymbol{\mu}_{\mathbf{h}}, \boldsymbol{\Sigma}_{\mathbf{h}})$, $V_k \sim VG^1(\beta_k, \mu_{h_k}, \Sigma_{h_k})$, $k = 1, \dots, n$, are independent, and

$$\boldsymbol{\mu}_{\mathbf{h}} = a \frac{\boldsymbol{\mu} \diamond \boldsymbol{\alpha} + (\boldsymbol{\Sigma} \diamond \boldsymbol{\alpha})\mathbf{h}}{K_{\mathbf{h}}}, \quad \boldsymbol{\Sigma}_{\mathbf{h}} = a \frac{\boldsymbol{\Sigma} \diamond \boldsymbol{\alpha}}{K_{\mathbf{h}}}, \quad (4.5)$$

$$\begin{aligned}
K_{\mathbf{h}} &= 1 - \langle \boldsymbol{\mu} \diamond \boldsymbol{\alpha}, \mathbf{h} \rangle - \frac{\|\mathbf{h}\|_{\boldsymbol{\Sigma} \diamond \boldsymbol{\alpha}}^2}{2}, \\
\mu_{h_k} &= \alpha_k \beta_k \frac{\mu_k + \Sigma_{kk} h_k}{K_{h_k}}, \quad \Sigma_{h_k} = \alpha_k \beta_k \frac{\Sigma_{kk}}{K_{h_k}}, \\
K_{h_k} &= 1 - \alpha_k \mu_k h_k - \frac{\alpha_k \Sigma_{kk} h_k^2}{2},
\end{aligned} \quad (4.6)$$

and

$$\mathcal{D}_{\mathbf{Z}} = \mathcal{D}_{\mathbf{V}_0} \cap \bigcap_{i=1}^n \mathcal{D}'_{V_k},$$

$$\mathcal{D}'_{V_k} := \{\boldsymbol{\theta} = (\theta_1, \dots, \theta_n) \in \mathbb{R}^n : \theta_k \in \mathcal{D}_{V_k}\}.$$

Proof. This follows from Corollary 4.2 with the representation $\mathbf{Z} \sim VGC_{n+1}^n$ from (2.6)–(2.8). \square

Remark 4.4. From Corollary 4.3, the k th marginal component has law

$$Z_k \stackrel{D}{=} \eta_k I + [\mathbf{V}_0]_k + V_k \quad (4.7)$$

under $\mathbb{Q}_{\mathbf{h}}$, where

$$[\mathbf{V}_0]_k \sim VG^1(a, [\boldsymbol{\mu}_\mathbf{h}]_k, [\boldsymbol{\Sigma}_\mathbf{h}]_{kk}), \quad V_k \sim VG^1(\beta_k, \mu_{h_k}, \Sigma_{h_k}), \quad (4.8)$$

are independent. Since Z_1 is a sum of 2 independent univariate VG processes, it is in general not a univariate VG process.

One way to see this is to take the example $n = 2$, $a = 0.5$, $\boldsymbol{\alpha} = (1, 1)$, $\boldsymbol{\mu} = \boldsymbol{\eta} = \mathbf{0}$, $\boldsymbol{\Sigma}$ as the identity matrix, and $\mathbf{h} = (1, 0.5) \in \mathcal{D}_\mathbf{Z}$. Assume for the purpose of contradiction that $Z_1 \sim VG^1(b, \mu, \Sigma)$ under $\mathbb{Q}_\mathbf{h}$ for some (b, μ, Σ) , which can be obtained by matching the first 3 central moments with those obtained from (4.8). Then $\nu := 1/b$ can be found in closed form by solving a quadratic equation, giving $\nu = 1.03788$ or 3.30906 , so that $\text{Kurt}_{\mathbb{Q}_\mathbf{h}}(Z_1) = 6.11364$ or 12.92718 . On the other hand, (4.8) implies $\text{Kurt}_{\mathbb{Q}_\mathbf{h}}(Z_1) = 9/2$, a contradiction. Thus, since a WVAG process must have VG marginal components, this shows the class of WVAG processes is not closed under the Esscher transform.

Relatedly, it should be noted that the \mathbb{Q}_{h_1} -dynamics of Z_1 from the Esscher transform of Z_1 is not necessarily the same as the $\mathbb{Q}_\mathbf{h}$ -dynamics of Z_1 from the Esscher transform of \mathbf{Z} . For example, if $Z_1 \sim VG^1$ under \mathbb{P} , then when $n = 1$, $Z_1 \sim VG^1$ under \mathbb{Q}_{h_1} , but this may be false when $n \geq 2$ since h_2, \dots, h_n generally, not just h_1 , affects the law of Z_1 under $\mathbb{Q}_\mathbf{h}$. \square

4.3 Analytical formula for cgf of the log return

Using the above results on the Esscher transform, we now obtain analytical formulas for the cgf of the log return in terms of the analytical formula in Theorem 3.3.

Let the time to maturity be $\tau := T - t$. We write the energy price process in the form $\mathbf{S}(T) = \mathbf{S}(t) \exp(\mathbf{R}(t, T))$, where the log return over $[t, T]$ is

$$\mathbf{R}(t, T) = \boldsymbol{\Lambda}(T) + \mathbf{X}(t)e^{-\lambda\tau} - \mathbf{Y}(t) + \mathbf{Z}^*(t, T)e^{-\lambda\tau}$$

and $\mathbf{X}(t) = \boldsymbol{\Lambda}(t) - \log \mathbf{S}(t)$. Using fact that $\mathbf{Z}^*(t, T)$ is independent of \mathcal{F}_t , and (2.10), the conditional distribution of $\mathbf{R}(t, T) | \mathcal{F}_t$ is

$$\mathbf{R}(t, T) | \mathcal{F}_t \stackrel{D}{=} \boldsymbol{\Lambda}(T) + \mathbf{X}(t)e^{-\lambda\tau} - \mathbf{Y}(t) + \mathbf{Z}^*e^{-\lambda\tau} \quad (4.9)$$

for some random vector $\mathbf{Z}^* \stackrel{D}{=} \mathbf{Z}^*(\tau)$ independent of \mathcal{F}_t . Let $\kappa_{\mathbf{R}(t, T)}^{\mathbb{Q}_\mathbf{h}}(\boldsymbol{\theta}) := \kappa_{\mathbf{R}(t, T) | \mathcal{F}_t}^{\mathbb{Q}_\mathbf{h}}(\boldsymbol{\theta})$ denote the cgf of this conditional distribution.

Proposition 4.5. *Using the setting and notation of Corollary 4.2, suppose $\mathbf{Z} \sim VG C_m^n(\mathbf{b}, \boldsymbol{\mu}, \boldsymbol{\Sigma}, \boldsymbol{\eta})$ under \mathbb{P} and $\mathbf{h} \in \mathcal{D}_\mathbf{Z}$. Then*

$$\kappa_{\mathbf{R}(t, T)}^{\mathbb{Q}_\mathbf{h}}(\boldsymbol{\theta}) = \langle \boldsymbol{\Lambda}(T) + \mathbf{X}(t)e^{-\lambda\tau} - \mathbf{Y}(t), \boldsymbol{\theta} \rangle + \kappa_{\mathbf{Z}^*(\tau)}^{\mathbb{Q}_\mathbf{h}}(e^{-\lambda\tau} \boldsymbol{\theta}) \quad (4.10)$$

for $\boldsymbol{\theta} \in \mathcal{D}_\mathbf{Z}$, where

$$\kappa_{\mathbf{Z}^*(\tau)}^{\mathbb{Q}_\mathbf{h}}(\boldsymbol{\theta}) = i \langle (e^{\lambda\tau} - 1) \boldsymbol{\eta}, \boldsymbol{\theta} \rangle + \sum_{j=1}^m \kappa_{\mathbf{V}_j^*(\tau)}^{\mathbb{Q}_\mathbf{h}}(\boldsymbol{\theta}), \quad (4.11)$$

and the law of \mathbf{V}_j , $j = 1, \dots, m$, under $\mathbb{Q}_{\mathbf{h}}$ is given in Corollary 4.2, and $\kappa_{\mathbf{V}_j^*}^{\mathbb{Q}_{\mathbf{h}}(\tau)}$ is evaluated by (3.3). Furthermore, (4.10) holds for $\boldsymbol{\theta} \in \mathbb{C}^n$ such that $\text{Re}(\boldsymbol{\theta}) \in \mathcal{D}_{\mathbf{Z}}$.

Proof. By (4.9), we have

$$\mathbb{E}_{\mathbb{Q}_{\mathbf{h}}}[e^{\langle \boldsymbol{\theta}, \mathbf{R}(t, T) \rangle} | \mathcal{F}_t] = e^{\langle \boldsymbol{\Lambda}(T) + \mathbf{X}(t)e^{-\lambda\tau} - \mathbf{Y}(t), \boldsymbol{\theta} \rangle} \mathbb{E}_{\mathbb{Q}_{\mathbf{h}}}[e^{\langle e^{-\lambda\tau} \boldsymbol{\theta}, \mathbf{Z}^*(\tau) \rangle}],$$

which is finite by the assumption that $\boldsymbol{\theta} \in \mathcal{D}_{\mathbf{Z}}$ which is equivalent to $e^{-\lambda\tau} \boldsymbol{\theta} \in \mathcal{D}_{\mathbf{Z}^*(\tau)}$. Thus, we obtain (4.10). Next, (4.11) follows from Corollary 4.2, which gives the law of \mathbf{Z} under $\mathbb{Q}_{\mathbf{h}}$, and (2.13) which gives the cgf of the corresponding $\mathbf{Z}^*(\tau)$. Lastly, $\kappa_{\mathbf{R}(t, T)}^{\mathbb{Q}_{\mathbf{h}}}$ can be analytically continued by the exponential moment theorem for all $\boldsymbol{\theta} \in \mathbb{C}^n$ such that $\text{Re}(\boldsymbol{\theta}) \in \mathcal{D}_{\mathbf{Z}}$. \square

Corollary 4.6. *Using the setting and notation of Corollary 4.3, suppose $\mathbf{Z} \sim WVAG^n(a, \boldsymbol{\alpha}, \boldsymbol{\mu}, \boldsymbol{\Sigma}, \boldsymbol{\eta})$ under \mathbb{P} and $\mathbf{h} \in \mathcal{D}_{\mathbf{Z}}$. Then $\kappa_{\mathbf{R}(t, T)}^{\mathbb{Q}_{\mathbf{h}}}(\boldsymbol{\theta})$ follows (4.10) for $\boldsymbol{\theta} = (\theta_1, \dots, \theta_n) \in \mathcal{D}_{\mathbf{Z}}$, where*

$$\kappa_{\mathbf{Z}^*(\tau)}^{\mathbb{Q}_{\mathbf{h}}}(\boldsymbol{\theta}) = i\langle (e^{\lambda\tau} - 1)\boldsymbol{\eta}, \boldsymbol{\theta} \rangle + \kappa_{\mathbf{V}_0^*}^{\mathbb{Q}_{\mathbf{h}}}(\boldsymbol{\theta}) + \sum_{i=1}^n \kappa_{V_k^*}^{\mathbb{Q}_{\mathbf{h}}}(\theta_k)$$

where the law of \mathbf{V}_0, V_k , $k = 1, \dots, n$, under $\mathbb{Q}_{\mathbf{h}}$ as given in Corollary 4.3, and $\kappa_{\mathbf{V}_0^*}^{\mathbb{Q}_{\mathbf{h}}}, \kappa_{V_k^*}^{\mathbb{Q}_{\mathbf{h}}}$ are evaluated by (3.3). Furthermore, (4.10) holds for $\boldsymbol{\theta} \in \mathbb{C}^n$ such that $\text{Re}(\boldsymbol{\theta}) \in \mathcal{D}_{\mathbf{Z}}$.

Proof. This follows from Proposition 4.5 and Corollary 4.3. \square

Proposition 4.7. *Using the setting and notation of Corollary 4.2, suppose $\mathbf{Z} \sim VGC_m^n(\mathbf{b}, \boldsymbol{\mu}, \boldsymbol{\Sigma}, \boldsymbol{\eta})$ under \mathbb{P} and $\mathbf{h} \in \mathcal{D}_{\mathbf{Z}}$. Then $V_{jk} := [\mathbf{V}_0]_k \sim VG^1([\mathbf{b}_{\mathbf{h}}]_j)_k, [[\boldsymbol{\mu}_{\mathbf{h}}]_j]_k, [[\boldsymbol{\Sigma}_{\mathbf{h}}]_j]_{kk}$, $j = 1, \dots, m$, and*

$$\kappa_{\mathbf{R}_k(t, T)}^{\mathbb{Q}_{\mathbf{h}}}(\theta) = (\Lambda(T) + X_k(t)e^{-\lambda\tau} - Y_k(t))\theta + \kappa_{Z_k^*}^{\mathbb{Q}_{\mathbf{h}}}(e^{-\lambda\tau}\theta) \quad (4.12)$$

for $\theta \in \mathbb{R}$ such that $\theta \mathbf{e}_k \in \mathcal{D}_{\mathbf{Z}}$, where

$$\kappa_{Z_k^*(T)}^{\mathbb{Q}_{\mathbf{h}}}(\theta) = (e^{\lambda T} - 1)\eta_k\theta + \sum_{j=1}^m \kappa_{V_{jk}^*}^{\mathbb{Q}_{\mathbf{h}}}(T)(\theta),$$

and $\kappa_{V_{jk}^*}^{\mathbb{Q}_{\mathbf{h}}}(T)$ is evaluated by (3.7). Furthermore, (4.12) holds for $\theta \in \mathbb{C}$ such that $\text{Re}(\theta)\mathbf{e}_k \in \mathcal{D}_{\mathbf{Z}}$.

Proof. The proof follows from similar arguments as the proof of Proposition 4.5, noting that $\kappa_{Z_k^*(\tau)}^{\mathbb{Q}_{\mathbf{h}}}(\theta) = \kappa_{\mathbf{Z}^*(\tau)}^{\mathbb{Q}_{\mathbf{h}}}(\theta \mathbf{e}_k)$. \square

Corollary 4.8. *Using the setting and notation of Corollary 4.3, suppose $\mathbf{Z} \sim WVAG^n(a, \boldsymbol{\alpha}, \boldsymbol{\mu}, \boldsymbol{\Sigma}, \boldsymbol{\eta})$ under \mathbb{P} and $\mathbf{h} \in \mathcal{D}_{\mathbf{Z}}$. Then $V_{0k} := [\mathbf{V}_0]_k$ and V_k satisfies (4.8), and $\kappa_{\mathbf{R}_k(t, T)}^{\mathbb{Q}_{\mathbf{h}}}(\theta)$ follows (4.12) for $\theta \in \mathbb{R}$ such that $\theta \mathbf{e}_k \in \mathcal{D}_{\mathbf{Z}}$, where*

$$\kappa_{Z_k^*(T)}^{\mathbb{Q}_h}(\theta) = (e^{\lambda T} - 1)\eta_k\theta + \kappa_{V_{0k}^*(T)}^{\mathbb{Q}_h}(\theta) + \kappa_{V_k^*(T)}^{\mathbb{Q}_h}(\theta),$$

and $\kappa_{V_{0k}^*(T)}^{\mathbb{Q}_h}, \kappa_{V_k^*(T)}^{\mathbb{Q}_h}$ are evaluated by (3.7). Furthermore, (4.12) holds for $\theta \in \mathbb{C}$ such that $\text{Re}(\theta)\mathbf{e}_k \in \mathcal{D}_Z$.

Proof. This follows from Proposition 4.7 and Corollary 4.3. \square

Note that following all the substitutions, all the cgfs $\kappa_{\mathbf{R}(t,T)}^{\mathbb{Q}_h}, \kappa_{R_k(t,T)}^{\mathbb{Q}_h}$ presented in this section have analytical formulas in terms of the dilogrothim function.

4.4 Pricing energy derivatives

We now use the analytical formulas for the cgf of the log return from the previous section to obtain pricing formulas for forwards, calls, and spread options.

The current time is t , the maturity time of the derivative is T and the time to maturity is $\tau = T - t$. Recall that $\mathbf{Z} \sim VGC_m^n(\mathbf{b}, \boldsymbol{\mu}, \boldsymbol{\Sigma}, \boldsymbol{\eta})$ or $\mathbf{Z} \sim WVAG^n(a, \boldsymbol{\alpha}, \boldsymbol{\mu}, \boldsymbol{\Sigma}, \boldsymbol{\eta})$.

4.4.1 Forward prices

Let S_k be a univariate energy price which is the k th marginal component of \mathbf{S} . The following result gives an analytical formula for its forward price.

Proposition 4.9. *Suppose that $\mathbf{Z} \sim VGC_m^n(\mathbf{b}, \boldsymbol{\mu}, \boldsymbol{\Sigma}, \boldsymbol{\eta})$ or $\mathbf{Z} \sim WVAG^n(a, \boldsymbol{\alpha}, \boldsymbol{\mu}, \boldsymbol{\Sigma}, \boldsymbol{\eta})$ under \mathbb{P} , and assume $\mathbf{h}, \mathbf{e}_k \in \mathcal{D}_Z$. The forward price of S_k at time t with maturity time T is*

$$F_t = S_t \exp(\kappa_{R_k(t,T)}^{\mathbb{Q}_h}(1)), \quad t \in [0, T], \quad (4.13)$$

where $\kappa_{R_k(t,T)}^{\mathbb{Q}_h}$ and \mathcal{D}_Z are given by Proposition 4.7 or Corollary 4.8, respectively.

Proof. As $\mathbf{h} \in \mathcal{D}_Z$, the Esscher measure \mathbb{Q}_h exists. Then the forward price is

$$F_t = \mathbb{E}_{\mathbb{Q}_h}[S_k(T) | \mathcal{F}_t] = S_t \mathbb{E}_{\mathbb{Q}_h}[e^{R_k(t,T)} | \mathcal{F}_t].$$

which gives the result if the expectation is finite, and this is provided by $\mathbf{e}_k \in \mathcal{D}_Z$ by Proposition 4.7 or Corollary 4.8. \square

Figure 1 shows possible shapes of the forward curve, which may increase or decrease in the short run but tend to increase in the long run. This can be contrasted with the standard Black-Scholes model where the forward curve is $\tau \mapsto S_t e^{r\tau}$ or to those in [5, Figure 7] for wind power futures.

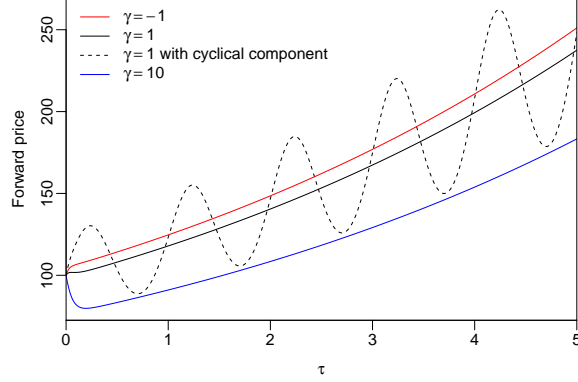


Figure 1: Forward price curve $\tau \mapsto F_8$ on S_1 , where the market price of risk is $\mathbf{h} = \gamma(-0.1, -0.03)$, $\gamma = -1, 1, 10$. All parameters are otherwise taken from Section 5.1 but $b_{21} = b_{31} = 0$ for all curves except the one with cyclical component.

4.4.2 Call options

Consider a call option on the univariate energy price S_k with strike price K and maturity time T . Suppose that $\mathbf{h}, (\epsilon + 1)\mathbf{e}_k \in \mathcal{D}_{\mathbf{Z}}$, then by the Carr-Madan formula [15], the price of the call option at time t is

$$c_t = C \int_0^\infty \operatorname{Re} \left(\frac{S_k(t)^{iv} K^{-iv} \exp(\kappa_{R_k}^{\mathbb{Q}_{\mathbf{h}}}(t, T)(\epsilon + 1 + iv))}{\epsilon^2 + \epsilon - v^2 + i(2\epsilon + 1)v} \right) dv, \quad t \in [0, T], \quad (4.14)$$

where

$$C = \frac{e^{-r(T-t)}}{\pi} K^{-\epsilon} S_k(t)^{\epsilon+1},$$

and $\epsilon > 0$ is the dampening parameter (α in [15]). Here, the cgf $\kappa_{R_k}^{\mathbb{Q}_{\mathbf{h}}}(t, T)(\theta)$ is obtained by Proposition 4.7 or Corollary 4.8 and its finiteness in the integrand is provided by $(\epsilon + 1)\mathbf{e}_k \in \mathcal{D}_{\mathbf{Z}}$. As usual, $\mathbf{h} \in \mathcal{D}_{\mathbf{Z}}$ is necessary for $\mathbb{Q}_{\mathbf{h}}$ to exist. Provided these conditions hold, ϵ has no effect on the call price. We make further comments on the choice of ϵ in Section 5.1.

Remark 4.10. Note that $(\epsilon + 1)\mathbf{e}_k \in \mathcal{D}_{\mathbf{Z}}$ is equivalent to $\mathbb{E}_{\mathbb{Q}_{\mathbf{h}}}[S_k^{\epsilon+1}] < \infty$, which is the necessary and sufficient condition for the Carr-Madan formula to be finite. For example, if the BDLP is $\mathbf{Z} \sim WVAG^n(a, \boldsymbol{\alpha}, \boldsymbol{\mu}, \boldsymbol{\Sigma}, \boldsymbol{\eta})$ then by combining bound for ϵ in [15, Section 5], Corollary 4.8, and (2.5), this is equivalent to

$$0 < \epsilon < \sqrt{\frac{\mu_k^2}{\Sigma_{kk}^2} + \frac{2}{\alpha_k \Sigma_{kk}}} - \frac{\mu_k}{\Sigma_{kk}} - 1$$

by noting that $(\epsilon + 1)\mathbf{e}_k \in \mathcal{D}_{\mathbf{V}_0}$ and $(\epsilon + 1)\mathbf{e}_k \in \mathcal{D}_{\mathbf{V}_k}$ turn out to be the same condition, and recalling the domain defined using the parameters under \mathbb{P} . \square

4.4.3 Spread options

Consider a spread option on the bivariate energy prices (S_k, S_l) , $k, l = 1, \dots, n$, $k \neq l$, with strike price K and maturity time T . By Remark 4.4, if $n \geq 3$, this is a more general setting with the possibility that the components \mathbf{h} other than the k th and l th component affect the law of (S_k, S_l) under $\mathbb{Q}_{\mathbf{h}}$.

Suppose that $\mathbf{h} \in \mathcal{D}_{\mathbf{Z}}$, then by the risk-neutral pricing formula, the price of the spread option at time t is

$$f_t((S_k, S_l)(t), K) := e^{-r(T-t)} \mathbb{E}_{\mathbb{Q}_{\mathbf{h}}} [(S_k(T) - S_l(T) - K)^+ | \mathcal{F}_t], \quad (4.15)$$

$t \in [0, T]$, expressed as a function of the current energy price $(S_k, S_l)(t)$ and strike price K , which is possible as the LDOUP is Markov and the option is path independent. Suppose also that $-\epsilon \in \mathcal{D}_{\mathbf{Z}}$, then the Hurd-Zhou formula [22] states that the price with strike 1 is

$$f_t((S_k, S_l)(t), 1) = \frac{e^{-rT}}{(2\pi)^2} \int_{\mathbb{R}^2} \exp(\kappa_{(R_k, R_l)(t, T)}^{\mathbb{Q}_{\mathbf{h}}}(-\epsilon + i\boldsymbol{\theta})) e^{\langle -\epsilon + i\boldsymbol{\theta}, \mathbf{Y}(t) \rangle} \hat{P}(\boldsymbol{\theta} + i\epsilon) d\boldsymbol{\theta}, \quad (4.16)$$

where

$$\hat{P}(\boldsymbol{\theta}) = \frac{\Gamma(i(\theta_k + \theta_l) - 1)\Gamma(-i\theta_l)}{\Gamma(i\theta_k + 1)}, \quad \boldsymbol{\theta} = (\theta_k, \theta_l),$$

Γ is the gamma function, and $\epsilon = (\epsilon_1, \epsilon_2)$ are dampening parameters that satisfy $\epsilon_1 + \epsilon_2 < -1$, $\epsilon_2 > 0$. Here, $\kappa_{(R_k, R_l)(t, T)}^{\mathbb{Q}_{\mathbf{h}}}(\boldsymbol{\theta})$ can be obtained by Proposition 4.5 or Corollary 4.6 by taking the k th and l th marginal component if $n \geq 3$ similar to Proposition 4.7, and its finiteness in the integrand is provided by $-\epsilon \in \mathcal{D}_{\mathbf{Z}}$. As before, provided these conditions hold, ϵ has no effect on the spread option price. Then the spread option price for a general strike price K is

$$f_t(S_k(t), S_l(t), K) = K f_t\left(\frac{(S_k, S_l)(t)}{K}, 1\right). \quad (4.17)$$

5 Implementation

We now outline for a specific choice of model how the pricing formulas in Section 4.4 can be applied in an end-to-end numerical implementation that includes simulating the model, fitting the model, and pricing spread options.

5.1 Model and parameter specification

Let $n = 2$ and suppose the energy spot price process $\mathbf{S}(t)$, $t \in [0, T_o]$ with terminal time $T = T_o$, is as specified in Section 4.1, where the LDOUP is $\mathbf{X} \sim OU - WVAG^2(\lambda, a, \alpha, \boldsymbol{\mu}, \boldsymbol{\Sigma}, \boldsymbol{\eta})$ with BDLP $\mathbf{Z} \sim WVAG^2(a, \alpha, \boldsymbol{\mu}, \boldsymbol{\Sigma}, \boldsymbol{\eta})$.

The risk-free rate is $r = 0.05$ and the period is $p = 1$. The *seasonality parameters* are $\mathbf{b} := (b_{01}, \dots, b_{31}, b_{02}, \dots, b_{32})$, where

$$(b_{01}, b_{11}, b_{21}, b_{31}) = (3.16132, 0.17500, 0.04385, 0.22986), \quad (5.1)$$

$$(b_{02}, b_{12}, b_{22}, b_{32}) = (2.04056, 0.31390, 0.01257, 0.06587). \quad (5.2)$$

The LDOUP parameters are $\vartheta := (a, \boldsymbol{\alpha}, \boldsymbol{\mu}, \boldsymbol{\Sigma}, \boldsymbol{\eta})$, where

$$\begin{aligned} \lambda = 18.25, \quad a = 3.15854, \quad \boldsymbol{\alpha} &= \begin{pmatrix} \alpha_1 \\ \alpha_2 \end{pmatrix} = \begin{pmatrix} 0.17183 \\ 0.28494 \end{pmatrix}, \\ \boldsymbol{\mu} = \begin{pmatrix} \mu_1 \\ \mu_2 \end{pmatrix} = \begin{pmatrix} -0.03071 \\ -0.20335 \end{pmatrix}, \quad \boldsymbol{\Sigma} = \begin{pmatrix} \Sigma_{11} & \Sigma_{12} \\ \Sigma_{12} & \Sigma_{22} \end{pmatrix} &= \begin{pmatrix} 0.24598 & 0.19452 \\ 0.19452 & 0.17045 \end{pmatrix}, \end{aligned} \quad (5.3)$$

and $\boldsymbol{\eta} = -\boldsymbol{\mu}$. We refer to the seasonality and LDOUP parameters together as the *model parameters*. It is necessary to choose $\boldsymbol{\eta}$ such that $\mathbb{E}[\mathbf{Z}(1)] = \bar{\boldsymbol{\mu}} = \mathbf{0}$ so that the model is identifiable, otherwise both $\boldsymbol{\eta}$ and the intercept (b_{10}, b_{20}) act as location parameters. Here, this choice is equivalent to $\boldsymbol{\eta} = -\boldsymbol{\mu}$. The initial value \mathbf{X}_0 is an independent random vector in the stationary distribution.

The market price of risk is

$$\mathbf{h} = \begin{pmatrix} h_1 \\ h_2 \end{pmatrix} = \begin{pmatrix} -0.1 \\ -0.03 \end{pmatrix},$$

which satisfies the necessary condition $\mathbf{h} \in \mathcal{D}_{\mathbf{Z}}$.

The current time is T_e , and \mathbf{S} has been observed in the time interval $t \in [0, T_e]$ with sampling interval Δ to estimate the model parameters. At time T_e , we price spread options which have strike prices K_i , $i = 1, \dots, 13$, which are equally spaced values from 0.4 to 10, and maturity time $T_o > T_e$, where the time to maturity is $\tau = T_o - T_e$. We set $T_e = 8$, $T_o = 8.5$, $\Delta = \frac{1}{250}$ with time measured in years. The current energy price is $\mathbf{S}(T_e) = (100, 96)$.

The Carr-Madan dampening parameter for call options on S_1 and S_2 is $\epsilon = 2.5$, which satisfies the conditions $(\epsilon + 1)\mathbf{e}_1, (\epsilon + 1)\mathbf{e}_2 \in \mathcal{D}_{\mathbf{Z}}$. The Hurd-Zhou dampening parameter is $\boldsymbol{\epsilon} = (\epsilon_1, \epsilon_2) = (-3.5, 1)$, which satisfies the conditions $\epsilon_1 + \epsilon_2 < -1$, $\epsilon_2 > 0$ and $-\boldsymbol{\epsilon} \in \mathcal{D}_{\mathbf{Z}}$.

Remark 5.1. In theory, any dampening parameter satisfying the above-mentioned condition has no effect on the call and spread option prices. In practical terms, when numerically evaluating the pricing formulas, we check that changing to nearby dampening parameters has virtually no effect, and any choice satisfying this will do. Further discussions on the choice of dampening parameter is given in [1, Section 4.2]. \square

5.2 Simulation

The observations of the LDOUP are $\mathbf{X}(t_i)$ $t_i = i\Delta$, $i = 0, 1, \dots, m$, where $m = \lfloor T_e/\Delta \rfloor = 2000$. These are simulated using the method in [24, Section 4.2] with $\tilde{n} = 1000$ subintervals. This means we use (2.11), where $\mathbf{Z}^*(\Delta)$ is simulated by discretizing the stochastic integral in (2.10) over $[0, \lambda\Delta]$ into \tilde{n} subintervals. Since the initial value \mathbf{X}_0 is assumed to be in its stationary distribution, which exists by [24, Proposition 1(i)], \mathbf{X}_0 is simulated by 20% burn-in.

5.3 Estimation

By (4.1), the seasonality parameters $(b_{0k}, b_{1k}, b_{2k}, b_{3k})$ are estimated with linear regression on the log price $Y_k(t_i)$, $i = 0, 1, \dots, m$, for each marginal component $k = 1, 2$. The estimation is valid since the errors are a zero mean stationary AR(1) process. Let the estimated seasonality parameters be $\widehat{\mathbf{b}} = (\widehat{b}_{01}, \dots, \widehat{b}_{31}, \widehat{b}_{02}, \dots, \widehat{b}_{32})$ and

$$\widehat{X}_k(t) = Y_k(t) - \left(\widehat{b}_{0k} + \widehat{b}_{1k}t + \widehat{b}_{2k} \cos\left(\frac{2\pi}{p}t\right) + \widehat{b}_{3k} \sin\left(\frac{2\pi}{p}t\right) \right), \quad k = 1, 2,$$

so that $(\widehat{X}_1(t_i), \widehat{X}_2(t_i)) = \mathbf{x}_i$, $i = 0, 1, \dots, m$, are the filtered observations of the LDOUP used to estimate $\boldsymbol{\vartheta}$ with the MLE method in [24].

Specifically, the likelihood function we use is $\boldsymbol{\vartheta} \mapsto L(\boldsymbol{\vartheta}, \mathbf{x}_0, \dots, \mathbf{x}_m)$, where

$$L(\boldsymbol{\vartheta}, \mathbf{x}_0, \dots, \mathbf{x}_m) = e^{mn\lambda\Delta} \prod_{k=1}^m f_{\mathbf{Z}^*(\Delta)}(e^{\lambda\Delta}\mathbf{x}_k - \mathbf{x}_{k-1}), \quad (5.4)$$

$f_{\mathbf{Z}^*(\Delta)}$ is the pdf of $\mathbf{Z}^*(\Delta)$, computed by taking the Fourier inversion of the characteristic function $\Phi_{\mathbf{Z}^*(\Delta)}(\boldsymbol{\theta}) = \exp(\kappa_{\mathbf{Z}^*(\Delta)}(\mathbf{i}\boldsymbol{\theta}))$, and $\kappa_{\mathbf{Z}^*(\Delta)}$ is given by Corollary 4.6. The numerical Fourier inversion method is described in [29, Section 4]. Using the notation there and in [24, Section 5.1], we set the number of grid points along each axis to be $N = 2^{12}$ for 1-dimensional FFT and $N = 2^8$ for 2-dimensional FFT, and the spacing h_k is chosen such that $\bar{x}_k = 30\sqrt{\text{Var}(Z_k^*(\Delta))}$, where $2\bar{x}_k$ is the width of the \mathbf{x} -grid along the \bar{x}_k axis on which the pdf is outputted. The factor $f_{\mathbf{x}(0)}(\mathbf{x}_0)$ has not been included in (5.4) as a single observation in the likelihood is negligible in practice for large sample sizes m , however to be more correct, [24] does include it and shows how it can be computed.

To estimate $\boldsymbol{\vartheta}$, we follow the 3-step procedure for the OU-WVAG process outlined in [24, Section 5.1], which estimates λ using method of moments on the lag 1 autocorrelation, the marginal parameters using MLE on the marginal components, and the joint parameters using MLE on the joint observations subject to a covariance constraint. Denote the estimated LDOUP parameters as $\widehat{\boldsymbol{\vartheta}}$.

Remark 5.2. In [24, Remark 9], it is noted that there was no known closed-form formula for $\Phi_{\mathbf{Z}^*(\Delta)}$ for a OU-WVAG process. We now have analytical formula and this substantially reduces the computational cost of MLE. While MLE can be used to estimate all parameters jointly by (5.4) and the analytical formula, with the 3-step procedure meant to be an approximation, it turns out the latter still performs better in practice as it allows a 1-dimensional FFT with large $N = 2^{12}$ to estimate the marginal parameters accurately at a low computational cost, while the former method may be limited to smaller N , such as $N = 2^8$, since 2-dimensional FFT has a higher computational cost. \square

5.4 Calibration

Next, we estimate the market price of risk \mathbf{h} , which is referred to as calibrating \mathbf{h} or calibrating the model. This is done by solving

$$\widehat{\mathbf{h}} = \arg \min_{\mathbf{h} \in \mathbb{R}^2} \sum_{i=1}^q (O_i - E_i)^2, \quad (5.5)$$

where O_i is the true price of the calibration instrument and E_i is the predicted price. The calibration instruments are forward or call prices on S_1 and S_2 observed at the current time T_e . For calibrating to the forward prices, the times to maturity, τ_i , $i = 1, \dots, 20$, are equally spaced values from 0.125 to 2.5. For calibrating to the call prices, the time to maturity is 0.5 and the strike prices, K_i , $i = 1 \dots, 20$, are equally spaced values from 25 to 175. Note that \mathbf{h} is estimated jointly over the calibration instruments on S_1 and S_2 , so $q = 40$.

The forward and call prices are computed using (4.13) and (4.14), respectively, where the true price uses the true parameters \mathbf{b} , $\boldsymbol{\vartheta}$ and the predicted price uses the estimated parameters $\widehat{\mathbf{b}}$, $\widehat{\boldsymbol{\vartheta}}$. To evaluate (4.14), we use numerical integration rather than FFT as done by Carr and Madan. A discussion on the improved accuracy and speed of this is given in [30, Section 15.2.3].

We refer to estimating the model parameters \mathbf{b} , $\boldsymbol{\vartheta}$ and calibrating \mathbf{h} jointly as fitting the model.

Remark 5.3. Our approach estimates $\boldsymbol{\vartheta}$ under \mathbb{P} and calibrates \mathbf{h} under $\mathbb{Q}_{\mathbf{h}}$. This is in contrast to other methods, such as in Gardini and Sabino [19], where the mean-correcting martingale measure is used. This requires that the model be specified under a risk-neutral measure \mathbb{Q} rather than \mathbb{P} , and then calibrated to forward and call prices. An issue then arises with the estimation of joint parameters, such as those affecting the correlation, which should be calibrated to the prices of other bivariate energy derivatives, but these may not be readily traded in the market, while estimating them using historical correlations under \mathbb{P} is inconsistent with the model. In contrast, our model combines both the observed energy prices \mathbf{S} under \mathbb{P} and univariate energy derivative prices to fit the model in a theoretically sound way. In fact, it is unclear whether this model can be estimated only by calibrating to derivative prices, as it may be the case that $\boldsymbol{\vartheta}$ and \mathbf{h} would become unidentifiable. This issue arises if energy prices follow the simpler Black-Scholes model.

Interestingly, h_2 affects the distribution of Z_1 under $\mathbb{Q}_{\mathbf{h}}$ as noted in Remark 4.4, so it seems possible in principle to calibrate \mathbf{h} to energy derivatives on S_1 only, which is not possible in the model of Gardini and Sabino. □

5.5 Pricing

Finally, we discuss the FFT method for numerically evaluating the spread option pricing formula in (4.16), which can be applied using the true or fitted model. While the implementation details are already given in [22] and also [1], here we provide additional explanation on how we obtain the spread option price for a panel of strike prices K_i , with a single FFT evaluation.

Consider a 2-dimensional grid in the $\boldsymbol{\theta}$ -domain and \mathbf{x} -domain. This is specified by N , the number of grid points along each axis, and $\bar{\theta}_k$, $k = 1, 2$, where

$2\bar{\theta}_k$ is the width of the grid along the θ_k -axis. If $\bar{\theta}_1 = \bar{\theta}_2$, denote this value by $\bar{\theta}$. The grid are matrices, which we denote with a minor abuse of notation also as $\boldsymbol{\theta} \in \mathbb{R}^{N \times N}$ and $\mathbf{x} \in \mathbb{R}^{N \times N}$, which have entries

$$\begin{aligned} [\boldsymbol{\theta}]_{\mathbf{i}} &= \left(\delta_{\theta_1} \left(-\frac{N}{2} + i_1 - 1 \right), \delta_{\theta_2} \left(-\frac{N}{2} + i_2 - 1 \right) \right), \quad \mathbf{i} = (i_1, i_2) \in \{1, \dots, N\}^2, \\ [\mathbf{x}]_{\mathbf{j}} &= \left(\delta_{x_1} \left(-\frac{N}{2} + j_1 - 1 \right), \delta_{x_2} \left(-\frac{N}{2} + j_2 - 1 \right) \right), \quad \mathbf{j} = (j_1, j_2) \in \{1, \dots, N\}^2, \end{aligned}$$

where the θ_k -spacing is $\delta_{\theta_k} = 2\bar{\theta}_k/N$ and the x_k -spacing is $\delta_{x_k} = 2\pi/(N\delta_{\theta_k})$ (note that $\bar{\theta}$, δ_{θ} , δ_x here are \bar{u} , η , η^* in [22]).

At the current time $t = T_e$, for the energy price $\mathbf{S}(t) = [\mathbf{x}]_{\mathbf{j}^*}$ on the \mathbf{x} -domain grid for some \mathbf{j}^* , it is shown in [22, Section 3] that, the price of the spread option is given by

$$f_t(\mathbf{S}(t), 1) \approx \frac{e^{-rT}}{(2\pi)^2} \delta_{\theta_1} \delta_{\theta_2} N^2 (-1)^{j_1^* + j_2^*} e^{-\langle \boldsymbol{\epsilon}, [\mathbf{x}]_{\mathbf{j}^*} \rangle} [\mathcal{F}^{-1}\{\mathbf{H}\}]_{\mathbf{j}^*} \quad (5.6)$$

where \mathcal{F}^{-1} is the normalized 2-dimensional discrete inverse Fourier transform and $\mathbf{H} \in \mathbb{C}^{N \times N}$ has entries

$$[\mathbf{H}]_{\mathbf{i}} = (-1)^{j_1 + j_2} \Phi([\boldsymbol{\theta}]_{\mathbf{i}} + i\boldsymbol{\epsilon}) \hat{P}([\boldsymbol{\theta}]_{\mathbf{i}} + i\boldsymbol{\epsilon}).$$

The approximation improves by taking a large N and $\bar{\theta}$.

Now suppose we want to price the spread option for a general strike price $K > 0$ using (4.17), then we require $\mathbf{S}(t)/K = [\mathbf{x}]_{\mathbf{j}}$ hold for some \mathbf{j} , that is, it is on the \mathbf{x} -grid. If $\mathbf{S}(t)/K$ is bounded by the \mathbf{x} -grid but not on it, taking the nearest grid point can lead to sizable pricing errors, so other approaches are considered.

1. Using bicubic interpolation of the \mathbf{x} -grid to compute to $f_t(\mathbf{S}(t)/K, 1)$.
2. Adjust the \mathbf{x} -grid so that $\mathbf{S}(t)/K$ is on it. Do this by setting \mathbf{j}^* as the index of the grid point nearest $\mathbf{S}(t)/K$, and then adjust the values of $\delta_{\theta_1}, \delta_{\theta_2}$ such that $\mathbf{S}(t)/K = [\mathbf{x}]_{\mathbf{j}^*}$ holds.

To compute the price of a spread option $f_t(\mathbf{S}(t), K_i)$ for a panel of strike prices K_i , $i = 1, \dots, q$, on a single FFT evaluation, we do both. For a particular strike price of K , we adjust the \mathbf{x} -grid so that $\mathbf{S}(t)/K$ is on it. Then a single FFT evaluation outputs $(f_t([\mathbf{x}]_{\mathbf{j}}, 1)) \in \mathbb{R}^{N \times N}$, from which we obtain $f_t(\mathbf{S}(t)/K_i, 1)$ using bicubic interpolation. Finally, $f_t(\mathbf{S}(t), K_i) = K_i f_t(\mathbf{S}(t)/K_i, 1)$ by (4.17). The grid is always adjusted so that $K = 3.6$ is on it.

Remark 5.4. Note that the FFT method for spread option pricing is different from the Fourier inversion method for estimation. The former uses the discrete inverse Fourier transform, while the latter uses the discrete Fourier transform. \square

Lastly, pricing spread options using the Monte Carlo method requires simulating $\mathbf{X}(T_o)$ conditional on $\mathbf{X}(T_e) = \log \mathbf{S}(T_e) - \boldsymbol{\Lambda}(T_e)$. This is done by either discretizing the SDE (1.2) or discretizing the integral $\mathbf{Z}^*(\tau)$ in (4.9), where we use $\tilde{n} = 10^5$ subintervals for both.

6 Numerical results

We now present numerical results on option pricing in our model based on the implementation details in Section 5. Results in Sections 6.1–6.2 are under the true model. Results in Sections 6.3–6.4 are from a simulation study using fitted models.

6.1 Spread option pricing under true parameters

Using the true parameters, Table 1 gives the spread option price using the FFT method with $N = 2^{11}$ grid points along each axis and $\bar{\theta} = 80$, and the Monte Carlo method with $N = 10^6$ simulations and $\tilde{n} = 10^5$ subintervals.

K_i	FFT	Monte Carlo	95% confidence interval
0.4	9.31079	9.32370	(9.28429, 9.36311)
1.2	9.03505	9.04812	(9.00917, 9.08708)
2.0	8.76650	8.77975	(8.74125, 8.81826)
2.8	8.50503	8.51849	(8.48044, 8.55655)
3.6	8.25053	8.26418	(8.22657, 8.30179)
4.4	8.00289	8.01663	(7.97947, 8.05379)
5.2	7.76200	7.77583	(7.73911, 7.81255)
6.0	7.52773	7.54163	(7.50535, 7.57790)
6.8	7.29998	7.31393	(7.27808, 7.34977)
7.6	7.07861	7.09258	(7.05717, 7.12799)
8.4	6.86350	6.87758	(6.84261, 6.91256)
9.2	6.65454	6.66877	(6.63422, 6.70332)
10.0	6.45158	6.46594	(6.43181, 6.50006)

Table 1: Spread option price over various strike prices K_i using the FFT method with $N = 2^{11}$, $\bar{\theta} = 80$ and the Monte Carlo method with $N = 10^6$ and $\tilde{n} = 10^5$.

This shows the spread option price using the FFT method closely agrees with the Monte Carlo method over the panel of strike prices. The 95% confidence intervals are also given, which is narrow due to the large number of simulations, with all prices from the FFT method within it.

For the Monte Carlo method, while simulating the integral should be more accurate than the SDE when it can be done exactly (for example, the model in [24, Section 3.1]), the choice is less clear when the integral also needs to be discretized. In this example, for small $\tilde{n} = 10^2$, the average error is 0.67664 for discretizing the integral and 0.3700 for the SDE, both upward biased with the true price outside the 95% confidence intervals in all cases. But for large $\tilde{n} = 10^5$, there is no significant difference. In our simulation, the average absolute difference between the prices of the two discretization methods is 3.1×10^{-4} , well within any difference detectable by the 95% confidence intervals in Table 1. Thus, we conclude that discretizing the SDE is more accurate and less biased than discretizing the integral, particularly for small \tilde{n} , while the difference is

negligible for large \tilde{n} .

Next, the average error over the panel of strike prices is defined as

$$\text{Average error} = \frac{1}{q} \sum_{i=1}^q |O_i - E_i|,$$

where O_i is the true price of the spread option with strike price K_i , and E_i is the price of the spread option computed in another way. We take the true price to be from the FFT method with $N = 2^{11}$, $\bar{u} = 80$, and it is compared with using the discretization parameters $N = 2^k$, $k = 6, 7, \dots, 10$, $\bar{\theta} = 40, 80$. Figure 2 shows how this affects the average error of the FFT method.

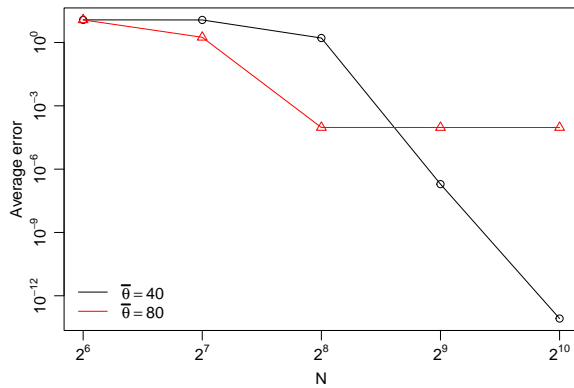


Figure 2: Average error using the FFT method for $N = 2^k$, $k = 6, 7, \dots, 10$, and $\bar{\theta} = 40, 80$. The plot is on a log scale.

The points in Figure 2 with large error only occur for small N , and in fact include situations for small K_i , where the spread option price is negative, or where no appropriate choice of ϵ in the sense of Remark 5.1 can be readily found. But as N and $\bar{\theta}$ increase, the average error vanishes, as expected. We see that $N = 2^8$, $\bar{\theta} = 40$ is enough to produce highly accurate results with average error in the order of 10^{-5} . Furthermore, the way the error reduces and flattens out is consistent with [22, Figures 1–3].

6.2 Spread option parameter sensitivities

Figure 3 shows the effect of the LDOUP parameters on the spread option price with strike price $K = 3.6$ and all others held constant. The parameters $a, \alpha_1, \alpha_2, \Sigma_{12}$ are plotting over their full range subject to the parameter constraints, the same is also true for the lower limit of Σ_{11}, Σ_{22} .

The spread option price decreases as the rate of mean reversion λ increases, as this reduces variability. The plots for the kurtosis parameters α_1 and α_2 have a point of nondifferentiability at $\alpha_2 = \alpha_1$ due to

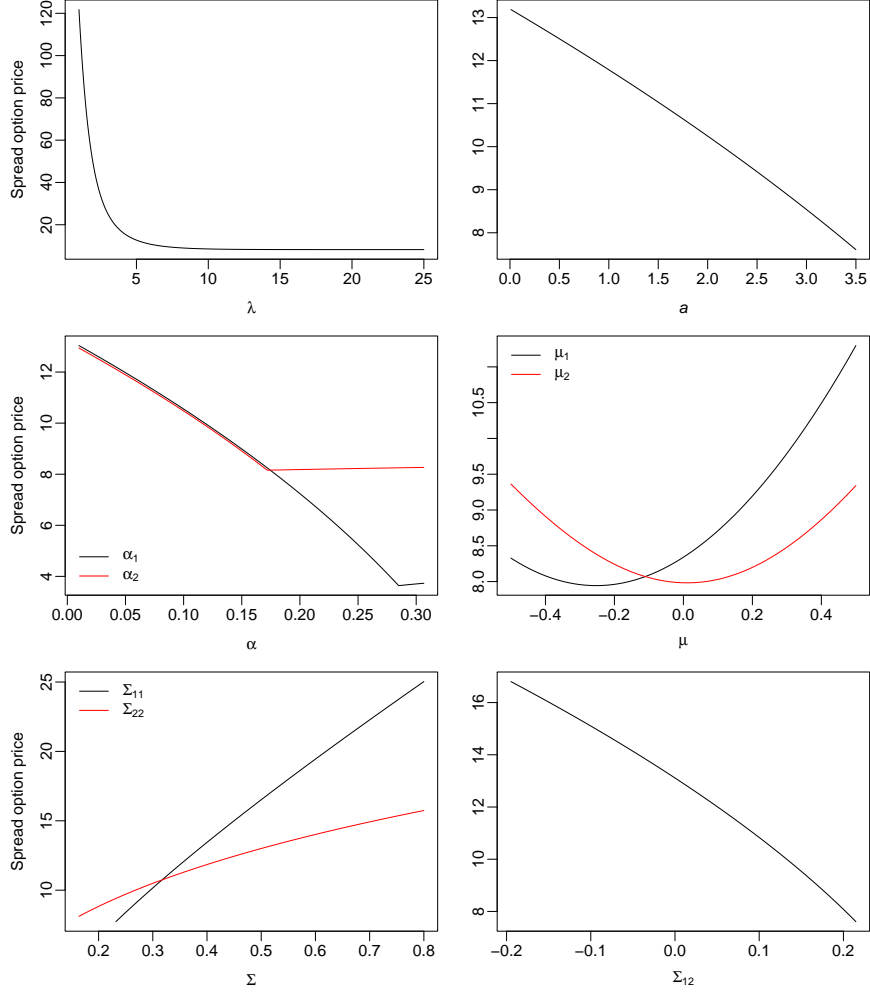


Figure 3: Spread option price with $K = 3.6$ as a function of the LDOUP parameters.

$$\text{Cov}_{\mathbb{Q}_h}(X_1(T_o), X_2(T_o) | \mathcal{F}_{T_e}) = \frac{1}{2}(1 - e^{-2\lambda\tau})a((\alpha_1 \wedge \alpha_2)\Sigma_{12} + \alpha_1\alpha_2\mu_1\mu_2).$$

As $\alpha_2 < \alpha_1$ decreases, the covariance decreases causing the price to increase, while as $\alpha_2 > \alpha_1$ increases, the covariance increases but the slope is near zero because $\mu_1\mu_2$ is as well. Some parameters may have surprising effects given that they affect moments other than what is considered their primary one. For example, it may be expected that increasing the skewness parameters μ_1 and μ_2 have opposite effects, but actually both tend to increase the variance of the

spread under $\mathbb{Q}_{\mathbf{h}}$ in asymmetric ways, which causes the price to increase. As Σ_{22} increases, this increases the variance of the spread because Σ_{11}, Σ_{12} are held constant, but ρ is not, and hence the price increases.

6.3 Fitting the model

We consider a simulation study based on 1000 simulated sample paths. Recalling the details from Section 5, each sample path has 2001 observations for estimating the model parameters, and 20 forward prices or call prices for calibration.

For 1 of the 1000 simulations, Figures 4 and 5 plot the log price sample path $Y_k(t)$, and compare the true and estimated seasonality function $\Lambda_k(t)$, as well as the true and fitted conditional distribution of the log returns $R_k(T_e, T_o) | \mathcal{F}_{T_e}$ under $\mathbb{Q}_{\mathbf{h}}$ for $k = 1, 2$. Define the risk-neutral drift as $\tilde{\boldsymbol{\mu}} = (\tilde{\mu}_1, \tilde{\mu}_2)$, where

$$\begin{aligned} \tilde{\mu}_k &:= \mathbb{E}_{\mathbb{Q}_{\mathbf{h}}}[R_k(T_e, T_o) | \mathcal{F}_{T_e}] \\ &= \Lambda_k(T_o) + X_k(T_e)e^{-\lambda\tau} - Y_k(T_e) + (1 - e^{-\lambda\tau})(\eta_k + [\boldsymbol{\mu}_{\mathbf{h}}]_k + \mu_{h_k}), \end{aligned}$$

$k = 1, 2$, due to (4.9) and (4.7), and this is shown in Figure 5.

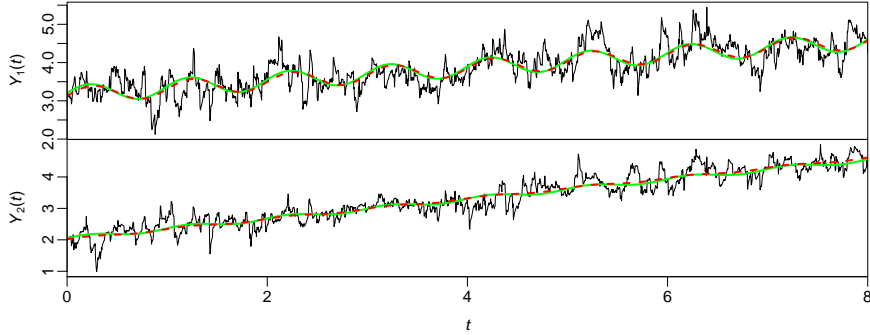


Figure 4: Sample path of the log price $Y_k(t)$ (black), true seasonality function $\Lambda_k(t)$ (green) and estimated seasonality function $\hat{\Lambda}_k(t)$ (red) for $k = 1, 2$

In both Figures 4 and 5, the true and estimated quantities are close, although the fitted distribution of $R_2(T_e, T_o)$ appears to have slightly lower variance than the true distribution, while the risk-neutral drifts are virtually identical.

Table 2 gives the true value, mean estimate, estimated standard error, and estimated relative root mean square error (RRMSE) of the seasonal parameters \mathbf{b} , LDOUP parameters $\boldsymbol{\vartheta}$, market prices of risk $\mathbf{h}^f = (h_1^f, h_2^f)$ and $\mathbf{h}^c = (h_1^c, h_2^c)$ from calibrating to forward and call prices, respectively, and their corresponding risk-neutral drifts $\tilde{\boldsymbol{\mu}}^f = (\tilde{\mu}_1^f, \tilde{\mu}_2^f)$, $\tilde{\boldsymbol{\mu}}^c = (\tilde{\mu}_1^c, \tilde{\mu}_2^c)$

From these results, most model parameters are estimated with moderately low RRMSE of approximately 10–30% other than those with true values near 0. Related to this, note that errors in estimating the model parameters are

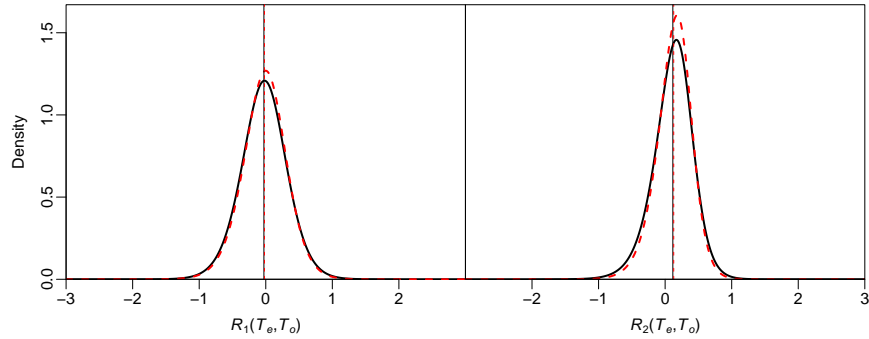


Figure 5: True (black) and estimated (red) pdf of $R_k(T_e, T_o) | \mathcal{F}_{T_e}$ under $\mathbb{Q}_{\mathbf{h}}$ and the corresponding means $\tilde{\mu}_k$ (vertical line) for $k = 1, 2$.

compensated for by the calibration. For instance, h_1^c and h_2^c have RRMSEs of 589% and 2612%, which can take them far from their true value, so that $\tilde{\mu}_1^c$ and $\tilde{\mu}_2^c$ can have small RRMSEs of 49% and 12%, close to their true value. In fact, on an absolute scale as seen by the vertical line in Figure 5, the differences between the true and estimated values of $\tilde{\mu}_1^c$ and $\tilde{\mu}_2^c$ are negligible. Ultimately, it is $\tilde{\boldsymbol{\mu}}$ that has a first-order effect on the energy derivative prices, and the fitted models should primarily be judged on how accurately it prices spread options.

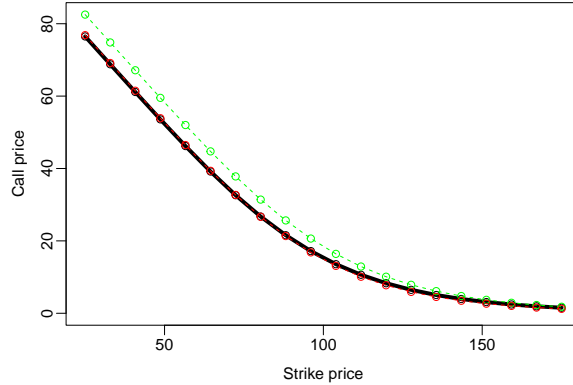


Figure 6: The true price of call options on S_1 (black), and based on estimated model parameters, the call price using the true market price of risk \mathbf{h} (green), using the estimated market price of risk $\hat{\mathbf{h}}^c$.

Figure 6 shows the results of calibrating to call prices. Based on the estimated model parameters, the estimated value $\hat{\mathbf{h}}^c$ yields a very close fit to the true prices of call options on S_1 , but the true value \mathbf{h} does not. While Figures 5 and 6 are based on a single simulation, these are typical results seen in most.

Parameter	True value	Mean estimate	Standard error	RRMSE (%)
b_{01}	3.16132	3.16012	0.08181	2.58672
b_{11}	0.17500	0.17512	0.01737	9.91921
b_{21}	0.04385	0.04453	0.05355	122.08732
b_{31}	0.22986	0.22998	0.05593	24.32271
b_{02}	2.04056	2.03718	0.07231	3.54595
b_{12}	0.31390	0.31433	0.01534	4.88649
b_{22}	0.01257	0.01236	0.04685	372.67504
b_{32}	0.06587	0.06285	0.04746	72.15719
λ	18.25000	19.72150	1.88547	13.10125
a	3.15854	3.78378	0.48648	25.07668
α_1	0.17183	0.16369	0.01692	10.91866
α_2	0.28494	0.23210	0.02699	20.82233
μ_1	-0.03071	-0.03114	0.01511	49.19107
μ_2	-0.20335	-0.18828	0.03601	19.19018
Σ_{11}	0.24598	0.22352	0.02720	14.33557
Σ_{22}	0.17045	0.14425	0.02185	20.00932
Σ_{12}	0.19452	0.16270	0.02204	19.89720
h_1^f	-0.10000	-0.10641	0.60613	605.86493
h_2^f	-0.03000	0.02163	0.80818	2698.06830
h_1^c	-0.10000	-0.09548	0.58939	589.11447
h_2^c	-0.03000	0.05402	0.77961	2612.46743
$\tilde{\mu}_1^f$	-0.02806	-0.02576	0.05889	209.91514
$\tilde{\mu}_2^f$	0.11560	0.12043	0.04996	43.40160
$\tilde{\mu}_1^c$	-0.02806	-0.02021	0.01131	49.05332
$\tilde{\mu}_2^c$	0.11560	0.12612	0.00985	12.46426

Table 2: True value, mean estimate, standard error, and RRMSE for the seasonal parameter, LDOUP parameters, market prices of risk, risk-neutral drifts estimated over 1000 simulation with 2001 observations and 20 calibration instruments per simulation.

Only results for calibrating to call prices on S_1 are plotted, although we calibrated to call prices on S_1 and S_2 . A similarly close match holds for call prices on S_2 , while calibration to forwards does not produce such a close match.

6.4 Spread option pricing under the fitted model

Finally, over the 1000 simulations, the results from using the fitted model to price spread options are presented in Table 3, with the calibration to forward and call prices shown separately. The spread option prices are computed by the FFT method with $N = 2^8$, $\bar{u} = 40$, which gives sufficient accuracy as noted in Section 6.1. The mean price and its RRMSE are given.

The results show that the spread options are priced less accurately when calibrated to forwards, with an average RRMSE of 30.8%, than to calls, where

K_i	True price	Calibrated to forwards		Calibrated to calls	
		Mean fitted price	RRMSE (%)	Mean fitted price	RRMSE (%)
0.4	9.31079	8.34185	28.87673	8.14641	16.05140
1.2	9.03506	8.07630	29.19487	7.88303	16.37409
2.0	8.76650	7.81817	29.51487	7.62714	16.69879
2.8	8.50502	7.56764	29.83218	7.37888	17.02162
3.6	8.25053	7.32462	30.14680	7.13819	17.34162
4.4	8.00290	7.08870	30.46282	6.90463	17.66241
5.2	7.76200	6.85969	30.77809	6.67802	17.98405
6.0	7.52774	6.63787	31.08973	6.45865	18.30082
6.8	7.29998	6.42256	31.40161	6.24581	18.61972
7.6	7.07862	6.21396	31.71286	6.03969	18.93635
8.4	6.86350	6.01140	32.02554	5.83965	19.25737
9.2	6.65454	5.81541	32.33447	5.64619	19.57346
10.0	6.45158	5.62567	32.64130	5.45901	19.88679

Table 3: Spread option price for the fitted models and their RRMSE over various strike prices K_i computed by the FFT method with $N = 2^8$, $\bar{\theta} = 40$. The true prices are from Table 1.

it is 18.0%. This shows how errors in fitting the model, from 2001 observations and 20 calibration instruments, propagate to pricing errors. As the sample size increases, so that the model parameters are estimated more accurately, the pricing error should approach 0.

It should be unsurprising that calibrating to calls leads to lower pricing error since the forwards calibrate over various maturities, whereas the calls calibrate to the same maturity and the different strikes, which implies out, in part, the marginal component and joint distribution of $\mathbf{S}(T_o) | \mathcal{F}_{T_e}$. Both calibration methods produce prices that are downward biased. Surprisingly, calibrating to calls has slightly larger bias and substantially lower standard error here.

7 Concluding remarks

The framework for pricing energy derivatives presented here has wider applicability beyond spread options. Following the explanations in Eberlein, Glau and Papapantoleon [17] and [23, 1], the FFT method can similarly be applied to other payoff functions with a known analytical Fourier transform. Moreover, clearly any European-style payoff in our model can be priced with the Monte Carlo method. Other extensions, such as generalizing the speed of mean reversion λ to a matrix, should also be possible, but are beyond the scope of this paper.

Appendix

A Choice of model parameters

The parameters in Section 5.1 are chosen to approximately resemble two examples of real data on energy prices appearing in the literature. The first marginal component based on the real data example in [8, Section 5.1], where $S(t)$ satisfies (4.1) with

$$\log S(t) = \Lambda(t) + X(t),$$

where $X(t)$ is a LDOUP $dX(t) - \lambda X(t)dt + d\tilde{Z}(t)$. The speed of mean reversion is $\tilde{\lambda} = 0.073$ under their time scale where $t = 250$ represents 1 year, and changing to our time scale where $t = 1$ does implies $\lambda = \tilde{\lambda}/\Delta$, where $\Delta = \frac{1}{250}$, with no change to the distribution of \tilde{Z} . This follows from the fact that if $\mathbf{X} \sim OU(\lambda, \mathbf{Z})$, then $(\mathbf{X}(ct))_{t \geq 0} \sim OU(c\lambda, \mathbf{Z})$ for $c > 0$. Thus, we obtain λ in (5.3).

The BDLP is a normal inverse Gaussian process $\tilde{Z} \sim \text{NIG}^1(\alpha, \beta, \gamma, \eta)$ with the usual parameterization (see [34, Section 5.3.8], η here is μ there). Specifically, their model has $(\alpha, \beta, \gamma) = (4.869, -0.125, 0.0874)$, and we set $\eta = 0.00284$ to make $\mathbb{E}[\tilde{Z}(1)] = 0$. The VG distribution that matches the 2nd, 3rd, 4th central moments is $\tilde{Z} \sim \text{VG}^1(0.42485, -0.00224, 0.01796)$. Finally, noting that $\tilde{Z} = Z(\lambda t)$, we obtain the parameter $\alpha_1, \mu_1, \Sigma_{11}$ in (5.3). Similarly, preliminary seasonality parameters (b_{01}, \dots, b_{31}) can be obtained to exactly match theirs, accounting for the change in time scale.

The second marginal component is based on the real data example in [9]. This model is $S(t) = \Lambda(t) + Y(t) + X(t)$, where Y is a NIG process and X is a OU-NIG process like in the first marginal component, where both NIG processes are independent. In particular, it is not of the form (4.1) and is an arithmetic model.

We simulate this model but deviate from [9] in a few ways. We change from their time scale where $t = 365$ represents 1 year to ours where $t = 1$ does, and take the sampling interval to be $\Delta = \frac{1}{250}$ as above. We set their parameter $\xi_0 = 40$, rather than 738.77, since this is approximately consistent with their plotted seasonality function, and set $\xi_4 = \xi_5 = 0$ to remove the weekend indicators. The simulation has 1001 observations, and is simulated until, like the real data, a completely positive sample path is obtained. Then we fit the marginal components of our model in Section 4.1 to this to obtain the parameters $\alpha_2, \mu_2, \Sigma_{22}$ in (5.3) and obtain preliminary estimates of the seasonal parameters (b_{20}, \dots, b_{23}) . Since the bivariate model for \mathbf{X} has only one λ , we use the value obtained from the first marginal component.

Energy prices tend to have very high correlation. Accordingly, the joint parameters a, Σ_{12} are chosen so that the Brownian motion correlation is $\rho = \Sigma_{12}/\sqrt{\Sigma_{11}\Sigma_{22}} = 0.95$, and $a = 0.9(\frac{1}{\alpha_1} \wedge \frac{1}{\alpha_2})$. Both are close to the maximum permitted by the parameter constraint $\rho \in (-1, 1)$ and $a \in (0, (\frac{1}{\alpha_1} \wedge \frac{1}{\alpha_2}))$, so that $\text{Corr}(Z_1(1), Z_2(1)) = 0.50303$ close to the maximum subject to the marginal

components specified above. To obtain a correlation approximately 1 for a WVAG process \mathbf{Z} would require both Z_1 and Z_2 to be approximately equal in law.

Finally, note that the cyclical component of the seasonality function $\Lambda_k(t)$ can be converted into the form

$$b_{2k} \cos\left(\frac{2\pi}{p}t\right) + b_{3k} \sin\left(\frac{2\pi}{p}t\right) = A \cos\left(\frac{2\pi(t - \phi)}{p}\right),$$

where A is the amplitude and $\phi \in [0, 1]$ is the phase. The phase is arbitrary and it is reasonable, but not necessary, to expect both energy prices have to have the same phase, so we convert the preliminary seasonal parameters to have $\phi = 0.22$ while keeping A unchanged. The intercept b_{0k} affects the price level and may also be considered arbitrary. We set it such that $\Lambda(T_e) = \log \mathbf{S}(T_e) = \log(100, 96)$, which is the current energy price. This choice corresponds to assuming $\mathbf{S}(T_e)$ is such that $\mathbf{X}(T_e)$ is at its stationary mean, with different choices of b_{0k} corresponding to assuming it is above or below that mean. This leads to seasonal parameters in (5.1)–(5.2).

The market price of risk being set to $\mathbf{h} = (-0.1, -0.03)$ is arbitrary but appears to be within the range of plausible values. See, for example, [5, Section 4.1] in the context of wind power futures.

Acknowledgments

Kevin Lu thanks Mesias Alfeus for discussions relating to this work.

References

- [1] M. Alfeus and E. Schlögl. On numerical methods for spread options. *FIRN Research Paper*, 2018.
- [2] L. Ballotta and E. Bonfigliani. Multivariate asset models using lévy processes and applications. *European Journal of Finance.*, 22(13):1320–1350, 2016.
- [3] H. Bauer. *Measure & Integration Theory*. Walter de Gruyter, Berlin, 1992.
- [4] F. E. Benth, J. Kallsen, and T. Meyer-Brandis. A non-Gaussian Ornstein-Uhlenbeck process for electricity spot price modeling and derivatives pricing. *Applied Mathematical Finance*, 14(2):153–169, 2007.
- [5] F. E. Benth and A. Pircalabu. A non-Gaussian Ornstein-Uhlenbeck model for pricing wind power futures. *Applied Mathematical Finance*, 25(1):36–65, 2018.
- [6] F. E. Benth and J. Šaltytė-Benth. The normal inverse Gaussian distribution and spot price modelling in energy markets. *International Journal of Theoretical and Applied Finance*, 7(2):177–192, 2004.

- [7] F. E. Benth and J. Šaltytė-Benth. Analytical approximation for the price dynamics of spark spread options. *Studies in Nonlinear Dynamics and Econometrics*, 10(3), 2006.
- [8] F. E. Benth, J. Šaltytė Benth, and S. Koekebakker. *Stochastic modelling of electricity and related markets*. World Scientific, 2008.
- [9] F. E. Benth and M. D. Schmeck. Pricing futures and options in electricity markets. In Sofia Ramos and Helena Veiga, editors, *The Interrelationship Between Financial and Energy Markets*, pages 233–260. Springer, Berlin Heidelberg, 2014.
- [10] A. Bubna-Litic. *Multivariate Variance Gamma Processes and Option Pricing*. Australian National University, Honours Thesis, 2012.
- [11] B. Buchmann, B. Kaehler, R. Maller, and A. Szimayer. Multivariate subordination using generalised Gamma convolutions with applications to Variance Gamma processes and option pricing. *Stoch. Proc. Appl.*, 127(7):2208–2242, 2017.
- [12] B. Buchmann, K. W. Lu, and D. B. Madan. Weak subordination of multivariate Lévy processes and variance generalised gamma convolutions. *Bernoulli*, 25(1):742–770, 2019.
- [13] R. Caldana and G. Fusai. A general closed-form spread option pricing formula. *Journal of Banking & Finance*, 37(12):4893–4906, 2013.
- [14] R. Carmona and V. Durrleman. Pricing and hedging spread options. *SIAM Review*, 45(4):627–685, 2003.
- [15] P. Carr and D. Madan. Option valuation using the fast Fourier transform. *Journal of Computational Finance*, 2(4):61–73, 1999.
- [16] A. Cartea and M. G. Figueroa. Pricing in electricity markets: a mean reverting jump diffusion model with seasonality. *Applied Mathematical Finance*, 12(4):313–335, 2005.
- [17] E. Eberlein, K. Glau, and A. Papapantoleon. Analysis of Fourier transform valuation formulas and applications. *Applied Mathematical Finance*, 17(3):211–240, 2010.
- [18] T. Fung and E. Seneta. Modelling and estimation for bivariate financial returns. *International Statistical Review*, 78(1):117–133, 2010.
- [19] M. Gardini and P. Sabino. Exchange option pricing under variance gamma-like models. *Applied Mathematical Finance*, 29(6):494–521, 2022.
- [20] Hans U. Gerber and Elias S. W. Shiu. Option pricing by esscher transforms. *Transactions of Society of Actuaries*, 76:99–191, 1994.

- [21] F. Hubalek and C. Sgarra. Esscher transforms and the minimal entropy martingale measure for exponential Lévy models. *Quantitative Finance*, 6(2):125–145, 2006.
- [22] T. R. Hurd and Z. Zhou. A fourier transform method for spread option pricing. *SIAM Journal on Financial Mathematics*, 1(1):142–157, 2010.
- [23] Y. K. Kwok, K. S. Leung, and H. Y. Wong. Efficient options pricing using the fast Fourier transform. In J.-C. Duan, W. K. Härdle, and J. E. Gentle, editors, *Handbook of Computational Finance*, pages 579–604. Springer, 2011.
- [24] K. W. Lu. Calibration for multivariate Lévy-driven Ornstein-Uhlenbeck processes with applications to weak subordination. *Statistical Inference for Stochastic Processes*, 25:365–396, 2022.
- [25] E. Luciano and P. Semeraro. Multivariate time changes for Lévy asset models: characterization and calibration. *J. Comput. Appl. Math.*, 233(5):1937–1953, 2010.
- [26] D. B. Madan, P. P. Carr, and E. C. Chang. The variance gamma process and option pricing. *European Finance Review*, 2(1):79–105, 1998.
- [27] D. B. Madan and E. Seneta. The variance gamma (v.g.) model for share market returns. *The Journal of Business*, 63(4):511–524, 1990.
- [28] H. Masuda. On multidimensional Ornstein-Uhlenbeck processes driven by a general Lévy process. *Bernoulli*, 310(1):97–120, 2004.
- [29] M. Michaelsen and A. Szimayer. Marginal consistent dependence modeling using weak subordination for Brownian motions. *Quantitative Finance*, 18(11):1909–1925, 2018.
- [30] A. Pascucci. *PDE and Martingale Methods in Option Pricing*. Springer-Verlag Italia, 2011.
- [31] P. Sabino. Exact simulation of variance gamma-related OU processes: application to the pricing of energy derivatives. *Applied Mathematical Finance*, 27(3):207–227, 2020.
- [32] K. Sato. *Lévy Processes and Infinitely Divisible Distributions*. Cambridge University Press, Cambridge, 1999.
- [33] K. Sato and M. Yamazato. Stationary processes of Ornstein-Uhlenbeck type. In K. Itô and J. V. Prohorov, editors, *Probability Theory and Mathematical Statistics*, pages 541–551. Springer, Berlin, 1983.
- [34] W. Schoutens. *Lévy Processes in Finance: Pricing Financial Derivatives*. John Wiley & Sons Ltd., 2003.

- [35] A. N. Shiryaev. *Essentials of Stochastic Finance*. World Scientific Publishing, 1999.
- [36] L. Valdivieso, W. Schoutens, and F. Tuerlinckx. Maximum likelihood estimation in processes of Ornstein-Uhlenbeck type. *Statistical Inference for Stochastic Processes*, 12:1–19, 2009.
- [37] D. Zagier. The dilogarithm function. In P. Cartier, P. Moussa, B. Julia, and P. Vanhove, editors, *Frontiers in Number Theory, Physics, and Geometry II*, pages 3–65. Springer, 2007.